NUMERICAL INVESTIGATION OF HYDRAULIC CHARACTERISTICS OF LALELI DAM SPILLWAY AND COMPARISON WITH PHYSICAL MODEL STUDY

A THESIS SUBMITTED TO
THE GRADUATE SCHOOL OF NATURAL AND APPLIED SCIENCES
OF
MIDDLE EAST TECHNICAL UNIVERSITY

BY

ERAY USTA

IN PARTIAL FULLFILLMENT OF THE REQUIREMENTS
FOR
THE DEGREE OF MASTER OF SCIENCE
IN
CIVIL ENGINEERING

MAY 2014

Approval of the thesis:

NUMERICAL INVESTIGATION OF HYDRAULIC CHARACTERISTICS OF LALELI DAM SPILLWAY AND COMPARISON WITH PHYSICAL MODEL STUDY

submitted by **ERAY USTA** in partial fulfillment of the requirements for the degree of **Master Science in Civil Engineering Department, Middle East Technical University** by,

Prof. Dr. Canan Özgen
Dean, Graduate School of **Natural and Applied Sciences** _____

Prof. Dr. Ahmet Cevdet Yalçıner
Head of Department, **Civil Engineering** _____

Assoc. Prof. Dr. Mete Köken
Supervisor, **Civil Engineering Dept., METU** _____

Prof. Dr. İsmail Aydın
Co-Supervisor, **Civil Engineering Dept., METU** _____

Examining Committee Members

Prof. Dr. Burcu Altan Sakarya
Civil Engineering Dept., METU _____

Assoc. Prof. Dr. Mete Köken
Civil Engineering Dept., METU _____

Prof. Dr. İsmail Aydın
Civil Engineering Dept., METU _____

Assoc. Prof. Dr. Şahnaz Tiğrek
Civil Engineering Dept., METU _____

Özgün Güler, M.Sc.
İOG Engineering _____

Date: 28 May 2014

I hereby declare that all information in this document has been obtained and presented in accordance with academic rules and ethical conduct. I also declare that, as required by these rules and conduct, I have fully cited and referenced all material and results that are not original to this work.

Name, Last name: Eray USTA

Signature :

ABSTRACT

NUMERICAL INVESTIGATION OF HYDRAULIC CHARACTERISTICS OF LALELI DAM SPILLWAY AND COMPARISON WITH PHYSICAL MODEL STUDY

Usta, Eray

M.S., Department of Civil Engineering

Supervisor: Assoc. Prof. Dr. Mete Köken

May 2014, 79 Pages

Spillway is a hydraulic structure that is used to pass big discharges in flood times in a controlled manner and release surplus water that cannot be safely stored in the reservoir to downstream. During the design process of the spillways, determining of hydraulic behavior of these structures is a very significant issue for an accurate and optimum design. In this thesis, the objective is to investigate the hydraulic characteristics of the flow over Laleli dam spillway numerically and compare the results with physical model. Flow over Laleli dam spillway was modeled numerically in three dimensions based on the Volume of Fluid (VOF) technique using Flow 3D which is widely used in flow analysis as a commercially available computational fluid dynamics (CFD) program. The model solved the Reynolds Averaged Navier-Stokes (RANS) equations with the Renormalized Group Equations (RNG) turbulence model on body independent orthogonal fixed grid. Appropriate grid selection, mesh refinement process, pressure distribution over the spillway, air entrainment effect, scale effect and cavitation potential over the spillway were investigated during this study. The results indicate that a three-dimensional numerical spillway model can be rapid and practical tool in order to predict the hydraulic parameters of the spillway flow.

Keywords: Spillway, Volume of Fluid, Flow 3D, Orthogonal Fixed Grid, Cavitation

ÖZ

LALELİ BARAJI DOLUSAVAĞI HİDROLİK KARAKTERİSTİKLERİNİN SAYISAL OLARAK ARAŞTIRILMASI VE DENEY MODELİ İLE KARŞILAŞTIRILMASI

Usta, Eray
Yüksek Lisans, İnşaat Mühendisliği Bölümü
Tez Yöneticisi: Doç. Dr. Mete Köken

May 2014, 79 Sayfa

Dolusavak, taşkın zamanlarında büyük debileri kontrollü bir şekilde geçiren ve rezervuarda güvenli olarak depolanamayan fazla suyu mansap kısmına aktaran hidrolik yapıdır. Dolusavakların tasarım aşamasında, bu yapıların hidrolik davranışlarının belirlenmesi doğru ve optimum tasarım açısından çok önemli bir konudur. Bu tezin amacı, Laleli barajı dolusavağı hidrolik karakteristiklerinin sayısal olarak araştırılması ve sonuçlarını deney sonuçlarıyla karşılaştırmaktır. Laleli barajı dolusavağı üzerindeki akım sonlu hacimler tekniği ile dolusavak akımlarının analizinde yaygın olarak kullanılan hesaplamalı akışkanlar dinamiği programı Flow 3D ile modellenmiştir. Sayısal modelde RANS denklemleri RNG türbülans modeli kullanılarak, geometriden bağımsız ortogonal hesap hücreleri üzerinde çözülmüştür. Bu çalışma boyunca, uygun hesap ağı seçimi, hesap hücrelerinin rafine edilme işlemi, dolusavak üzerindeki basınç dağılımı, akıma hava girişi etkisi, ölçek etkisi ve dolusavaktaki kavitasyon durumu araştırılmıştır. Sonuçlar, üç boyutlu dolusavak sayısal modelinin, dolusavak üzerindeki akımın hidrolik parametrelerinin belirlenmesinde hızlı ve pratik bir araç olduğunu göstermiştir.

Anahtar Kelimeler: Dolusavak, Sonlu Hacimler Tekniği, Flow 3D, Ortogonal Hesap Hücreleri, Kavitasyon

To My Family

ACKNOWLEDGEMENTS

I wish to express my deepest gratitude to my supervisor Assoc. Prof. Dr. Mete Köken for his guidance, advice, criticism, encouragements and insight throughout the research. I would also like to thank to Prof. Dr. İsmail Aydın for his support and advice during this research. Finally, I would like to express my deepest appreciation to my family and friends for the support, understanding and motivation that they provided me throughout my life.

TABLE OF CONTENTS

ABSTRACT ..... **v**

ÖZ ..... **vi**

ACKNOWLEDGEMENTS ..... **viii**

TABLE OF CONTENTS ..... **ix**

LIST OF TABLES ..... **xi**

LIST OF FIGURES ..... **xii**

CHAPTERS

1. INTRODUCTION **1**

1.1 Definition of the Problem *1*

1.2 Research Objectives *5*

2. LITERATURE REVIEW **7**

2.1 Numerical Studies *7*

2.2 Experimental Investigations Over Laleli Dam Spillway *12*

2.2.1 Description of Model 12

2.2.2 Test Facilities 13

2.2.3 Model Operation 15

2.2.4 Evaluations of Experimental Study 19

3. COMPUTATIONAL TOOL **21**

3.1 General Process of Performing a CFD Analysis *21*

3.2 Introduction to Flow 3D *24*
3.2.1 Discretization Techniques 25

4. NUMERICAL MODEL IMPLEMENTATION **29**

4.1 Pre-Processor *29*
4.1.1 Geometric Representation 29
4.1.2 Grid Generation 31
4.1.3 Boundary and Initial Conditions 36
4.1.4 Physics 38
4.1.4.1 Turbulence Modeling 38
4.1.4.2 Air Entrainment Model 39
4.1.4.3 Gravity 39
4.1.5 Material Properties 41
4.2 Solver Options *41*

5. NUMERICAL SIMULATIONS RESULTS **43**

5.1 Grid Selection and Mesh Refinement *44*
5.1.1 Simulations for Case 1 46
5.1.2 Simulations for Case 2 52
5.2 Air Entrainment and Scale Effects *60*
5.3 Investigation of Cavitation Potential *64*

6. CONCLUSIONS **75**

REFERENCES **77**

LIST OF TABLES

TABLES

Table 2.1 Design Discharges of Laleli Dam.....13
Table 2.2 Dimensions of Aeration Ramps.....17
Table 3.1 Steps of a CFD Analysis.....23
Table 5.1 Scaling Ratios for Froude Similitude.....43
Table 5.2 Summary of Grid Generation Trials for Case 1..... 47
Table 5.3 Volume of Flow Rates for Case 1..... 48
Table 5.4 Summary of Grid Generation Trials for Case 2.....53
Table 5.5 Cavitation Indexes for NMR 8 Using Depth-Averaged Velocity.....69
Table 5.6 Section-Averaged Velocity Computation.....71
Table 5.7 Cavitation Indexes for NMR 8 Using Section-Averaged Velocity.....72

LIST OF FIGURES

FIGURES

Figure 1.1 Ogee-crested Spillway 2
Figure 2.1 Laleli Dam Spillway 12
Figure 2.2 Hydraulic Model of Laleli Dam Spillway 14
Figure 2.3 Detail of Hydraulic Model 15
Figure 2.4 The Design Parameters of Aeration Ramps 16
Figure 2.5 The Final Design Parameters of Aeration Ramp (TR-5) 18
Figure 2.6 The Hydraulic Model with Aeration Ramp (TR-5) 18
Figure 3.1 Grid System for Flow 3D (Flow 3D Advanced Hydraulic Training-2012) 24
Figure 3.2 General Solution Method for an Incompressible Flow (Flow 3D General Training Class-2013) 25
Figure 3.3 Control Volume Representation in Flow 3D (Flow 3D General Training Class-2013) 26
Figure 3.4 Sharp Interface of Fluid Fraction (Flow 3D Advanced Hydraulics Training-2013) 27
Figure 3.5 FAVOR (Introduction to Flow 3D for Hydraulics-2013) 28
Figure 4.1 Physical Model Geometry of Laleli Dam Spillway (TR-5) 30
Figure 4.2 Computational Domain of Case 1 32
Figure 4.3 Grid Generation of Case 1 32
Figure 4.4 Computational Domain of Case 2 33
Figure 4.5 Grid Generation of Case 2 34
Figure 4.6 Cell Aspect Ratio and Size Ratio (Flow 3D Lecture Notes) 35
Figure 4.7 Non-Uniform Grid Generation with 2 Mesh Planes 35
Figure 4.8 Initial Condition of Case 1 37
Figure 4.9 Initial Condition of Case 2 38

Figure 4.10 Gravity Vector For Case 1 40
Figure 4.11 Gravity Vector For Case 2 40
Figure 5.1 Measurement Points over the Physical Model 46
Figure 5.2 Comparison of Pressure Head Values Along The Measurement Points for NM 1 and Experiment 49
Figure 5.3 Comparison of Pressure Head Values Along The Measurement Points for NM 2 and Experiment 49
Figure 5.4 Comparison of Pressure Head Values Along The Measurement Points for NM 3 and Experiment 50
Figure 5.5 Comparison of Pressure Head Values Along The Measurement Points for NM 4 and Experiment 50
Figure 5.6 Comparison of Pressure Head Values Along The Measurement Points for NM 5 and Experiment 51
Figure 5.7 Comparison of Pressure Head Values Along The Measurement Points for NMR 1 and Experiment 54
Figure 5.8 Comparison of Pressure Head Values Along The Measurement Points for NMR 2 and Experiment 54
Figure 5.9 Comparison of Pressure Head Values Along The Measurement Points for NMR 3 and Experiment 55
Figure 5.10 Comparison of Pressure Head Values Along The Measurement Points for NMR 4 and Experiment 55
Figure 5.11 Comparison of Pressure Head Values Along The Measurement Points for NMR 5 and Experiment 56
Figure 5.12 Comparison of Pressure Head Values Along The Measurement Points for NMR 6 and Experiment 56
Figure 5.13 Comparison of Pressure Head Values Along The Measurement Points for NMR 7 and Experiment 57
Figure 5.14 Comparison of Pressure Head Values Along The Measurement Points for NMR 8 and Experiment 57

Figure 5.15 Comparison of Pressure Head Values Along The Measurement Points for NMR 9 and Experiment 58
Figure 5.16 2-D Pressure Contours at Central Axis of Spillway (NMR 8) 59
Figure 5.17 2-D Velocity Magnitude Contours at Central Axis of Spillway (NMR 8) 59
Figure 5.18 Comparison of Pressure Head Values Along The Measurement Points for NMR 8 with and without Air Entrainment Model 60
Figure 5.19 Comparison of Pressure Head Values Along The Measurement Points for NMR 8 in Model and Prototype Scale 61
Figure 5.20 Comparison of Pressure Head Values Along The Measurement Points for NMR 8 in Prototype Scale with and without Air Entrainment Model 62
Figure 5.21 Volume Fraction of Entrained Air in Model Scale 63
Figure 5.22 Volume Fraction of Entrained Air in Prototype Scale 63
Figure 5.23 Comparison of the Aeration (%) For NMR 8 in Model and Prototype Scale 64
Figure 5.24 Velocity Distribution at 23rd point (x-z plane) 66
Figure 5.25 Velocity Distribution at 27th point (x-z plane) 66
Figure 5.26 Velocity Distribution at 34th point (x-z plane) 67
Figure 5.27 Velocity Distribution at 37th point (x-z plane) 67
Figure 5.28 Velocity Distribution at 40th point (x-z plane) 68
Figure 5.29 Velocity Distribution at 42nd point (x-z plane) 68
Figure 5.30 Comparison of the Experimental and the Numerical Cavitation Index Values for TR-5 70
Figure 5.31 Comparison of the Depth-Averaged Velocity Values for TR-5 70
Figure 5.32 Comparison of the Section-Averaged Velocity Values for TR-5 72
Figure 5.33 Comparison of the Experimental and the Numerical Cavitation Index Values for TR-5 73

LIST OF SYMBOLS AND ABBREVIATIONS

A	The cross-sectional area of the spillway (m^2)
b	Width of spillway (m)
y	depth (m)
y_{av}	average depth (m)
g	Gravitational acceleration (m/s^2)
H_0	Design Head of spillway (m)
P	Pressure (Pa)
P_v	Vapor Pressure (Pa)
Q	Discharge (m^3/s)
V	Velocity (m/s)
γ	Unit Weight (N/m^3)
ρ	Density of fluid (kg/m^3)
σ	Cavitation Index
L_r	Length of aeration ramp (m)
t_r	Height of aeration ramp (m)
α	Angle between ramp and spillway chute (°)
l_r	Scaling Ratio for Froude Similitude

CHAPTER 1

INTRODUCTION

1.1 Definition of the Problem

Spillway is one of the most significant component of a dam to ensure the safety of the dam during the flood. It controls the flow and transfers the excess water from reservoir to tailwater for preserving dam against overtopping. According to the definition of United States Department of the Interior Bureau Reclamation (USBR), spillways are provided for storage and detention dams to release surplus water or floodwater that cannot be contained in the allotted storage space, and for diversion dams to bypass flows exceeding those turned into the diversion system. The flow regime upstream of the spillway is subcritical and the state of flow is supercritical at the spillway face. The identification of hydraulic characteristics for a spillway is difficult issue because of the rapidly varied flow type and the alternation in the state of flow from subcritical regime to supercritical regime. In the design of a spillway, the determination of discharge capacity should be investigated carefully because the main reason of failure of many dams is improperly design of the spillways.

There are several types of spillways but the most common type is the ogee-crested spillways because of their ability to release surplus water from upstream to downstream efficiently and safely when properly designed and implemented. These types of spillways, which are also called as the overflow spillways, have larger capacities, higher hydraulic conformities, and easily adaptable to all type of dams. The ogee-shape holds over the downstream side until it reaches the determined slope on the downstream face. This slope is maintained for the remainder of the spillway as far as the base of the dam and finally, the flow enters a suitable energy dissipating basin.

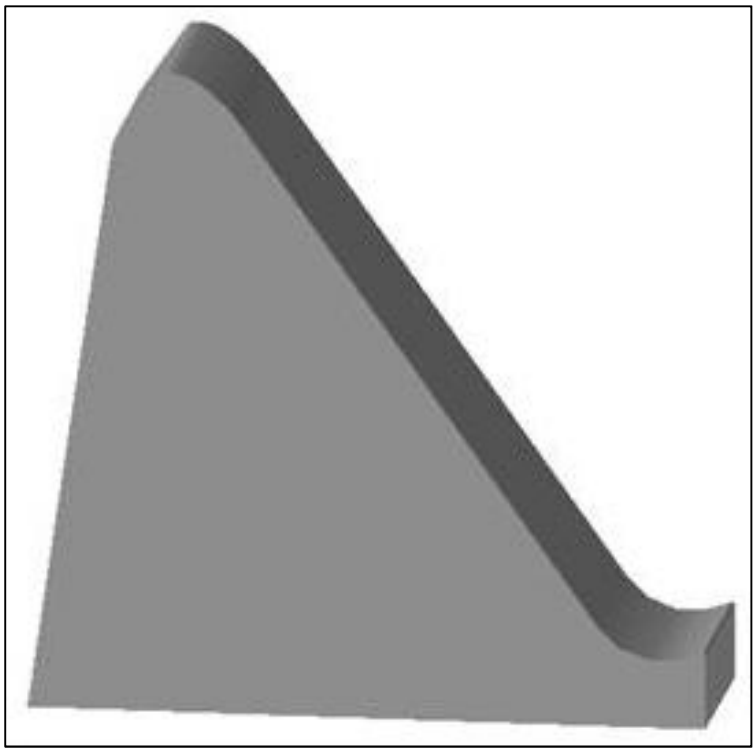

Figure 1.1 Ogee-crested Spillway

The theory of flow over a spillway is based largely upon empirical formulas, coefficients and design charts. A lot of investigations and model tests have been done to obtain empirical formulation for finding the hydraulic characteristics as spillway crest shapes, pressures and discharge coefficients by U.S Bureau of Reclamation (USBR) and U.S. Army Corps of Engineers (USACE). In practice, the design guidelines which has been formed by USBR and USACE for spillways consist of simplified flow situations and standard geometries. The design charts and empirical equations have been found as a result of the series of hydraulic model tests for designing spillways. However, the experimental models are only for certain types of spillways and only applicable for these types.

The shape of the crest is an important part of the hydraulic design of the spillway because of the bottom pressure distribution on the spillway face. While spillway is subjected to a flood, a strong curvature of streamlines is formed at the crest. The

internal pressure may decrease below atmospheric pressure so that overflowing water may desire to leave from the spillway face. It causes a vacuum effect at the separation point and a cavitation risk may take place. According to Falvey (Cavitation in Chutes and Spillways, 1990), cavitation is defined as the formation of a bubble or void within a liquid. The local pressure reductions associated with cavitation can be caused by turbulence or vortices in flowing water. It is the most common reason of serious damage to spillways and is affected by many factors such as flow rate, air flow rate, velocity, pressure and operation time. Spillways may be subjected to cavitation risk due to vaporization on the spillway face resulting from localized boundary shape conditions. In flowing water, if the pressure reduces down to the vapor pressure, bubbles or cavities would form locally in the body of flow due to flow separation. These bubbles are transported within the flow and when they reach to a region where pressure is sufficiently large they explode and cause serious damage on the structure.

The most effective method of preventing cavitation damage is to be aerated the flow along the flow boundary. To prevent cavitation, aeration ramps could be used at the spillway face in order to ventilate the flow. It is known that air ventilation decreases the tendency for cavitation. If the natural air entrainment is not sufficient for aeration, additional air could be introduced into the flow with the help of external aeration shafts. The purpose of the aeration is to increase the local pressure within the flow to atmospheric pressure. However, predicting the cavitation damage is a very difficult issue. On the other hand, estimating the inception point of the cavitation is much easier than calculating magnitude of the damage.

The complex phenomenon of spillway hydraulics has been studied mostly with hydraulic model experiments. In the design of spillways, physical models have been used for the accurate estimation of discharge capacity, discharge coefficient, local flow patterns, free surface profile, velocities, pressures, friction losses and investigation of cavitation risk. However, the physical model tests are very expensive, fairly time consuming and there are many uncertainties and difficulties

associated with the scaling effects. The recent development of computer technology has provided a solution to complicated hydraulic problems using various mathematical models. Computational Fluid Dynamics (CFD) is the numerical modeling method to analyze the fluid flow problems. Numerical models are usually much less time consuming than physical models. Furthermore, the computational cost of numerical models is low relative to the experimental tests. In a numerical model, changes in a design can be easily adopted to existing model. High-capacity computers and efficient CFD codes provide realistic fluid flow solutions so that CFD could be thought as virtual laboratory. Although the numerical model has a lot of advantages with respect to the physical model, it should be validated with the physical model results.

In this thesis, the commercially available CFD software, Flow 3D, is used to Laleli dam spillway by solving the Reynolds Averaged Navier-Stokes equations with the Renormalized Group Equations (RNG) as the turbulence closure. Several flow scenarios both in model and prototype scales are simulated in Flow 3D and the model scale results are compared with the data obtained from physical model tests of the Laleli dam spillway which was built with a scale of 1:25 in Middle East Technical University (METU) Hydromechanics Laboratory.

Laleli dam is located on the Coruh River in the North East of Turkey. This dam is the first dam at the upstream of Coruh River so that it is subjected to huge discharges. Type of the dam is roller compacted concrete (RCC) dam. Laleli dam's total spillway width is 38 m and it is controlled by four radial gates. The downstream channel of the spillway has a slope of 1.43. Laleli dam spillway ends with a flip bucket type of deflector. The elevation difference between spillway's crest and downstream end of flip bucket is 103.5 m. Due to the very steep channel and high velocities, Laleli dam has a cavitation risk. The experimental model studies were done in order to obtain the hydraulic characteristics of Laleli dam spillway and investigate the cavitation risk.

The software uses Volume of Fluid (VOF) method to track the free surface. Flow 3D makes it easy to generate rating curves and detailed velocity profiles for complex spillways, including the effects of air entrainment and transport. Flow 3D is widely used to confirm the hydraulic performance of proposed spillway designs and to help professionals meet dam safety requirements (www.flow3d.com). The numerical model simulations of Laleli dam spillway are completed in the scope of this thesis. The hydraulic parameters are obtained from simulations and compared the results with experimental study. Several different scenarios are performed and tried to find the most optimum and accurate solutions.

1.2 Research Objectives

Physical models have been used extensively in order to analyze flow over spillways as these structures are very important for the safety of dams and they have complicated hydraulic properties but there are significant disadvantages implementing the physical models. Most significant disadvantages of the physical model tests are high costs, limited information on the flow field, long time required to get the results and the possible scale effects that cannot be avoided. On the other hand, if an appropriate numerical model is used, one can get valuable flow information such as pressure, velocity, amount of air through the whole flow domain.

The main objective of this thesis is to investigate the flow parameters over a spillway using a three-dimensional numerical model. Flow characteristics such as flow rate, depths, water surface profiles, pressures on the ogee-crested spillway and downstream canal, vertical distributions of velocity are investigated both for model and prototype scale using commercial CFD code, Flow 3D. First, a validation is made comparing the numerical results with the experimental ones in the model scale. Second, the scale effects are investigated by making additional simulations in the prototype scale and comparing these with the model scale results. Moreover, air-entrainment model in Flow 3D is used to estimate the amount of air entrained as a

result of the aeration device installed on the spillway. As a final step, the cavitation potential of Laleli dam spillway is investigated.

CHAPTER 2

LITERATURE REVIEW

2.1 Numerical Studies

With the development of the computational power in the hydraulic engineering, numerical methods have been increasingly used in investigating the flow over spillways. After numerical models were validated with physical model tests and started to be used as a design tool.

Olsen and Kjellesvig (1998) modeled numerical water flow over a spillway in two and three dimensions for various geometries in order to estimate the spillway capacity. RANS equations were solved with k - ε turbulence model on a structured non-orthogonal grid. The results were compared with experimental study where there was a good agreement on discharge coefficient. Moreover, the pressure distribution on spillway was also acceptably closer to the physical model results.

Yakun, et al. (1998) presented a study about numerical modeling of spillway flow with a free drop and initially unknown discharge. Flows over different spillway profiles were studied. The discharge, profiles of the free drop and the pressure distributions on the walls were computed from the numerical model. The numerical results were in good agreement with the measured ones.

Unami, et al. (1999) solved a 2-D numerical spillway model to verify the applicability of the model to practical design. An unstructured triangular mesh system was used. Both finite element and finite volume methods were used for resolving of 2-D free surface flow equations. In addition to the flow equations, air entrainment model was also added to the system. The study proved that the model was valid as a primary analysis tool for hydraulic design of spillways.

Song and Zhou (1999) worked on a numerical approach in order to simulate and study the effect of geometry on the free surface flow over a tunnel spillway. The weakly compressible flow (compressible hydrodynamic model) equations were solved with an explicit finite volume method. Large Eddy Simulation (LES) was used as turbulence closure model where body fitted grid system was used. The computed time-averaged free surface profile, pressure and velocity distribution were compared with the measured values. It was concluded that 3-D free surface flow simulations can be made much more efficient than the usual incompressible flow approach by adopting the compressible hydrodynamic approach.

Savage and Johnson (2001) completed their study using Flow 3D in order to compare the flow parameters over a standard ogee-crested spillway between physical model test results, existing spillway literature design guidelines created by USACE and USBR and numerical simulation results. The numerical simulations were solved with Reynolds Averaged Navier-Stokes equations using finite volume method. This study showed that numerical tools were sufficiently advanced to calculate discharge and pressure on the spillway. Although physical model studies were still considered the basis from which other methods were compared, the numerical simulations had an improved accuracy over the design nomographs for obtaining the discharge capacities and pressures.

Teklemariam, et al. (2002) tried to apply Flow 3D in hydraulic engineering applications. As a result of case studies, CFD analysis provided a considerable design support for advanced hydraulic engineering projects. The CFD models were also used to provide insight into the planned physical models.

Ho, et al. (2003) investigated two and three dimensional CFD modeling of spillway behavior under rising flood levels. The results have been validated against published data and a good agreement was obtained.

Kim and Park (2005) analyzed the flow structure over ogee spillway in consideration of scale and roughness effects. The commercially available CFD package, Flow 3D

was used in this study. RANS equations were solved and RNG model was used as turbulence closure. It was obtained that numerical errors due to the roughness effects were insignificant and if the length scale ratio is less than 100 or 200, the scale effects of the model were in an acceptable error range.

Dargahi (2006) investigated the flow field over a spillway to simulate the flow by means of a three dimensional numerical model. In this study, boundary fitted coordinate system was created. In order to calculate the free surface flow over the spillway, volume of fluid (VOF) model was used. k - ε turbulence model was used where turbulent kinetic energy (k) and dissipation rate (ε) were obtained from experimental data. The numerical model was simulated under various head values. The results of simulations depended on the choice of the wall function, grid spacing and Reynolds number. The water surface profiles and the discharge coefficients were predicted with an accuracy range of 1.5 - 2.9 % depending on spillway's operating head.

Johnson and Savage (2006) showed the influence of the tailwater on the spillway. In 2001, Savage and Johnson investigated the flow parameters and compared the results of physical test studies, existing spillway literature design guidelines created by USACE and USBR and numerical model studies. This study was used in order to show that the pressure along the spillway under the submergence effect could be accurately predicted using numerical models. The comparison indicated that numerical modeling can estimate the flow rate and pressure distribution on the spillway accurately. Moreover, it was stated that numerical models can provide more details about velocity and pressure distribution than the physical models.

Bhajantri, et al. (2006) described the formulation and development of a two dimensional free surface flow numerical model for flow over a spillway. The objective of study was to investigate the hydraulic characteristics of the flow over the spillway. Pressures, velocities and other non-dimensional hydraulic parameters such as the Froude number and the cavitation index were analyzed. Simulations were

completed using inviscid weakly compressible flow equations. Numerical model results showed reasonable agreement with the results measured from the physical model tests.

Kim, et al. (2010) simulated the flow over Karin dam spillway using Flow 3D software. The rectangular coordinate system was defined and RANS equations were solved. After the simulation results were evaluated, there were some problems about the flow stability in approach channel so that some alterations were implemented about initial plan design. After the revised plan design was simulated, the results of the numerical model were compared with the physical model test and excellent agreement was observed between the numerical model and physical model. The results represented that the flow over the spillway was stable for revised design.

Jacobsen and Olsen (2010) investigated the capacity of a complex spillway and calculated the stage-discharge curve with a three dimensional numerical model solving RANS equations using finite difference method with the standard $k - \varepsilon$ turbulence model. A fixed orthogonal grid was used in the computations. The results were compared with a physical model study. The deviation between the computed and measured values of the rating curve was under 2% for most of the discharges whereas at some points it increased to a maximum value of 10% where the flow was most complex. As a result of the study, it is stated that the use of numerical modeling to compute spillway capacity caused considerable savings in both cost and time for hydraulic engineering design.

Zhenwei, et al. (2012) studied flow over a spillway using numerical model that utilizes VOF method with multidimensional two phase flow. The water flow in the whole spillway was simulated defining unstructured hexahedral grid using a $k - \varepsilon$ turbulence model. Numerical modeling results showed good agreement with experimental results in flow parameters such as free surface elevation, pressure and flow velocity. It was stated that the flow characteristics obtained from numerical analysis can provide detailed data for the design.

Morales, et al. (2012) analyzed free flow over the ogee shaped spillway with a tainter gate using a three dimensional finite volume code that used transient VOF method and k – ε turbulence model to capture the free surface profile. Also, physical model tests were done and compared with the numerical results. Most of the simulation results were in reasonable agreement with the physical model tests. This study showed that CFD can be use as a design tool for hydraulic structures.

Daneshkhah and Vosoughifar (2012) worked about the impacts of different turbulence models on flow parameters for ogee spillways using Fluent software. The results calculated by the numerical models were compared with the experimental results. RNG k – ε turbulence model showed more accurate results over ogee spillway.

Azmoudeh and Kamanbedast (2013) calculated the flow parameters using Flow 3D in order to determine appropriate location of the aeration system of the chute for preventing the cavitation risk. In this study, Gotvand dam's spillway and chute was worked as a case study. Cavitation numbers were computed by the numerical model and measured from the physical model at different locations of the aerator systems. A good agreement between the numerical and physical modes was obtained. It was found that total average difference between the results was 0.03% which was in acceptable range for a CFD analysis.

Singh, et al. (2013) presented a case study of iterative simulations of the flow over the spillway of Ratle Hydro Electric Project, for various modifications which were intended to obtain a hydraulic design, compatible with the topography on the downstream side. Physical model tests with a scale of 1:55 were also completed in the scope of this study. RANS equations were solved and RNG turbulence model was used as the closure model. As a result of this study, although the use of a coarse mesh caused errors in the discharge values, the trajectory of water was simulated quite accurately by Flow 3D.

2.2 Experimental Investigations Over Laleli Dam Spillway

2.2.1 Description of Model

The physical model of Laleli dam spillway in a scale of 1:25 was constructed in METU Hydromechanics Laboratory. The behavior of spillway was investigated against the flood discharges and the hydraulic parameters of the flow were obtained. Due to the fact that Laleli dam is the most upstream dam on the Coruh river, it could be subjected to high flood discharges. The maximum water level of Laleli dam is 1480 m and the crest level of the spillway is 1473.50 m. Spillway crest length is 38 m and it is controlled by four radial gates. The elevation difference between the crest of spillway and the downstream of the flip bucket deflector is 103.5 m. The slope of the spillway channel is 1.43. Because of the high downstream channel and high slope, a cavitation risk exists on the Laleli dam spillway. A scheme view of Laleli dam spillway is shown in Figure 2.1.

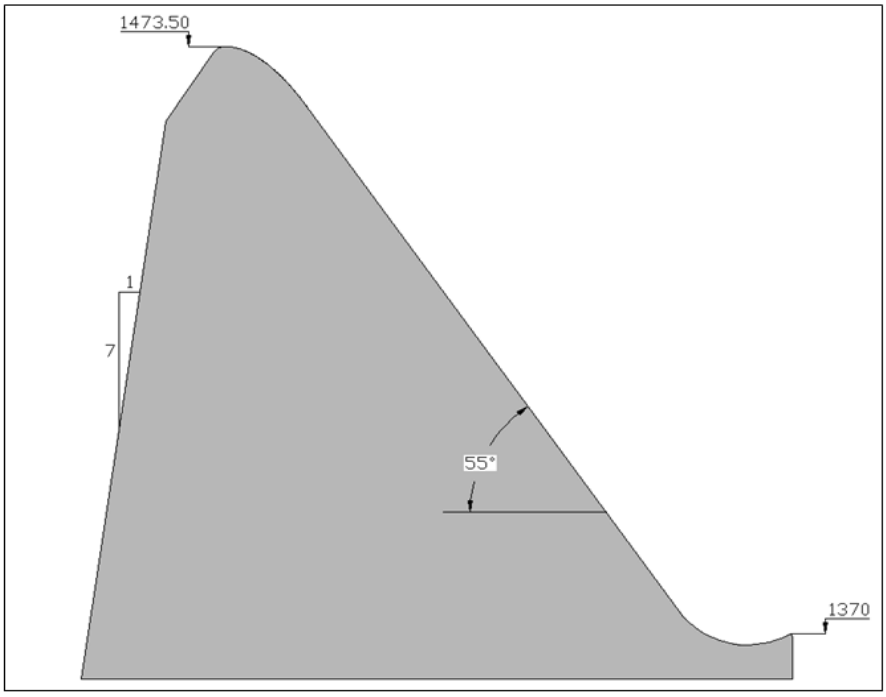

Figure 2.1 Laleli Dam Spillway

The entrance conditions, flow around the dividing walls, water depths and the pressure distributions all along the centerline of the spillway chute were investigated. In the hydraulic model, the similarity was achieved by Froude similarity law. The model scale of 1:25 was selected considering height of the spillway and 1000 years return period discharge, Q_{1000}. The half of the spillway was modeled. In order to obtain appropriate initial conditions, 600 m of the reservoir was symmetrically modeled as an approach channel. Design discharge values at different flood frequencies for Laleli dam is given in Table 2.1.

Table 2.1 Design Discharges of Laleli Dam

Flood Frequency (yrs)	**Symbol**	**Discharge (m^3/s)**
10000	Q_{10000}	1456
1000	Q_{1000}	1023
100	Q_{100}	591
50	Q_{50}	355
25	Q_{25}	229
10	Q_{10}	154

The Hydraulic Model Studies of Laleli Dam Spillway was reported by Aydın et al. (2012).

2.2.2 Test Facilities

At the entrance of the model reservoir, a filter was formed for absorbing the turbulence and jet effects of water which was conveyed by pipes. A brick wall was formed in front of the pipes which conveyed the water to reservoir in order to

regulate the flow and damp the oscillations. In the model, a full channel was placed in the middle and two half channels were symmetrically placed on both sides of the spillway chute to avoid sidewalls effects. At the end of the chute, a flip bucket deflector was set. The discharge of the model was measured using a rectangular sharp crested weir that was placed on the exit of the model. In order to measure the piezometric heads, piezometer tubes were placed on the central axis of the spillway at 53 points. Pressure heads were obtained over the centerline of the spillway chute using these piezometer tubes. The hydraulic model of Laleli dam spillway and detail of the hydraulic model are shown in Figure 2.2 and Figure 2.3 respectively.

Figure 2.2 Hydraulic Model of Laleli Dam Spillway

Figure 2.3 Detail of Hydraulic Model

2.2.3 Model Operation

Discharge capacity of the spillway was found and the stage – discharge curve was obtained for full gate opening. The piezometric heads were measured at the central axis of the spillway chute and flip bucket for different discharge values. The pressures on the spillway were generally positive but negative values were also measured at some points. In the flow direction, the first negative pressure was recorded close to the crest which did not cause any trouble due to low velocity values; however, negative pressure observed at the downstream (x = 27 m in prototype scale) could cause cavitation. Therefore, different aeration devices were tested to avoid cavitation.

In order to show the cavitation risk, the cavitation number (σ) could be calculated.

$$\pm = \frac{P - P_V}{\circ V^2} \tag{2.1}$$

P and P_v are the pressure and vapor pressure respectively; whereas ρ is the density of water and V is the average velocity of the fluid. The cavitation risk begins with the value of cavitation number less than 0.2.

TR-1 was the first scenario. The piers were lengthened to the end of the ogee crest shape and the sharp form was given to the piers. However, the desired pressure distribution was not obtained and the surface waves oscillations were not dampened. Moreover, cavitation number didn't change after the geometric alterations.

The scenarios of TR-2, TR-3 and TR-4 consisted of aeration ramps. The conceptual drawing of the aeration ramp is shown in Figure 2.4. The aeration ramp was placed at the end of the ogee crest shape. The piers were also lengthened till the end of the ogee crest shape.

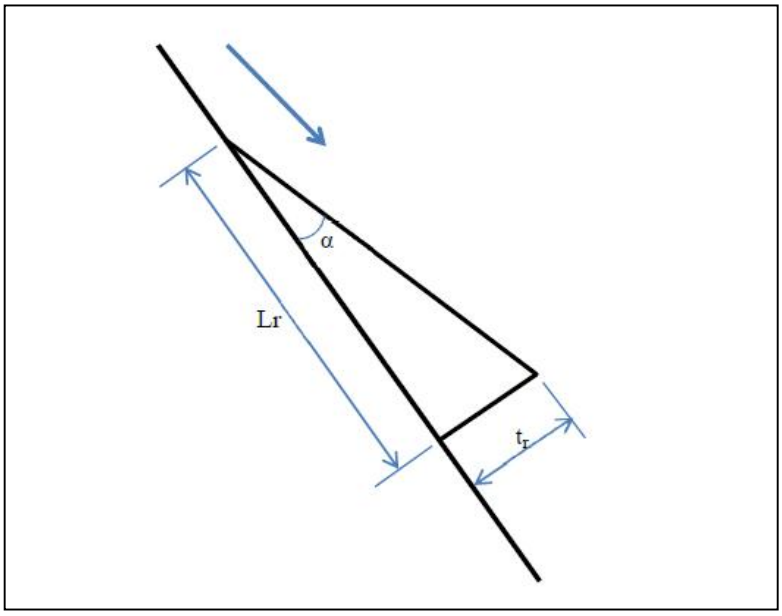

Figure 2.4 The Design Parameters of Aeration Ramps

Three different scenarios were investigated to determine the adequate ramp height and jet length. Dimensions of the aeration ramps tested are given in Table 2.2.

Table 2.2 Dimensions of Aeration Ramps

Design Number	**t_r (m)**	**L_r (m)**	**α °**
TR-2	0.60	4.20	8.21
TR-3	0.50	4.20	6.84
TR-4	0.40	4.20	5.47

For these scenarios, the aerator ramp eliminated the cavitation risk for the first half of the chute, on the other hand the second half of the chute still contained that the risk for discharges greater than Q_{100}. Therefore, it was decided to shift the aeration ramp at a further position in the downstream direction.

In the scenario TR-5, the aeration ramp was shifted towards a downstream section with a higher Froude number, thereby increasing both the ventilation and air mixture until the end of the chute protecting the spillway against the cavitation risk. In Figure 2.5, the final design parameters of the aeration ramp are shown.

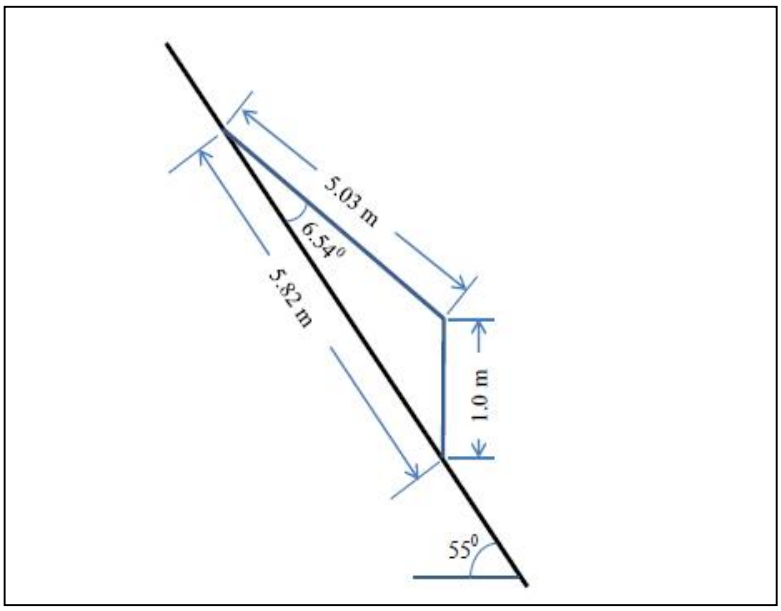

Figure 2.5 The Final Design Parameters of Aeration Ramp (TR-5)

The aeration ramp is represented over the hydraulic model in Figure 2.6.

Figure 2.6 The Hydraulic Model with Aeration Ramp (TR-5)

2.2.4 Evaluations of Experimental Study

The main purpose of this study was to obtain the hydraulic parameters of flow over Laleli dam spillway. There was not a problem with respect to hydraulic conformity at the entrance of the spillway. According to the experimental results, the capacity of spillway was sufficient to carry the flood discharges but a significant portion of the spillway chute was under the cavitation risk.

As a precaution against cavitation, aeration ramp which deflected the flow from spillway bottom surface was designed. Aeration ramp design parameters were researched and proper positioning of the ramp was investigated. The appropriate location was determined to be at x = 26 m in prototype scale. Ventilation in the spillway chute provided enough aeration until the end of the spillway.

CHAPTER 3

COMPUTATIONAL TOOL

3.1 General Process of Performing a CFD Analysis

Computational fluid dynamics is a tool for the investigation of systems relating fluid flow problems by means of computer-based simulation techniques. It is a method for simulating a flow process in which standard flow equations such as the Navier-Stokes and continuity equations are discretizated and solved at each computational cell. Although for most of the cases, CFD technique is very powerful and very cheap to perform, at the end of a simulation the user should evaluate the results. If the numerical model is not suitable for the problem investigated or the model is not set up correctly, then the results will not reflect the physical solutions. It is necessary to obtain experimental data comparisons with analytical solutions and similar works to validate the numerical simulation results. CFD codes could obtain the results in many ways at virtual environment. There are a lot of commercially available CFD packages. These packages have sophisticated user interfaces to define the flow domain and boundary conditions easily. All CFD codes generally contain three main stages. These stages are pre-processor, solver and post-processor stages respectively.

Pre-processing is generating the input parameters of a fluid flow problem to a CFD program by a user interface. The numerical modeling starts with a computational mesh. A number of interconnected elements are formed in the computational domain. In this stage, after the geometry and computational domain of the problem are defined, grid generation (mesh) is done. The grid generation is a very significant step because the accuracy of a numerical simulation depends on the grid quality. Within the pre-processing step fluid properties are also introduced and appropriate boundary conditions and initial conditions are specified

In the solver stage, discretizated forms of the governing equations of fluid flow over all the computational cells are solved. Each flow parameter is calculated at each computational cell.

A CFD simulation generates an enormous amount of data and it is not possible to post-process that manually. Many CFD packages have been developed with the visualization and post-processing tools, where a huge amount of data could be analyzed. There are also specialized post-processing softwares where 2D and 3D surface plots, vector plots, contour plots, iso-surfaces, flowlines, geometry and grid display, text data outputs and a lot of combination of graphs could be drawn. Moreover, they may also include animation tools for displaying dynamic results.

The steps of a CFD analysis can be listed as following Table 3.1.

Table 3.1 Steps of a CFD Analysis

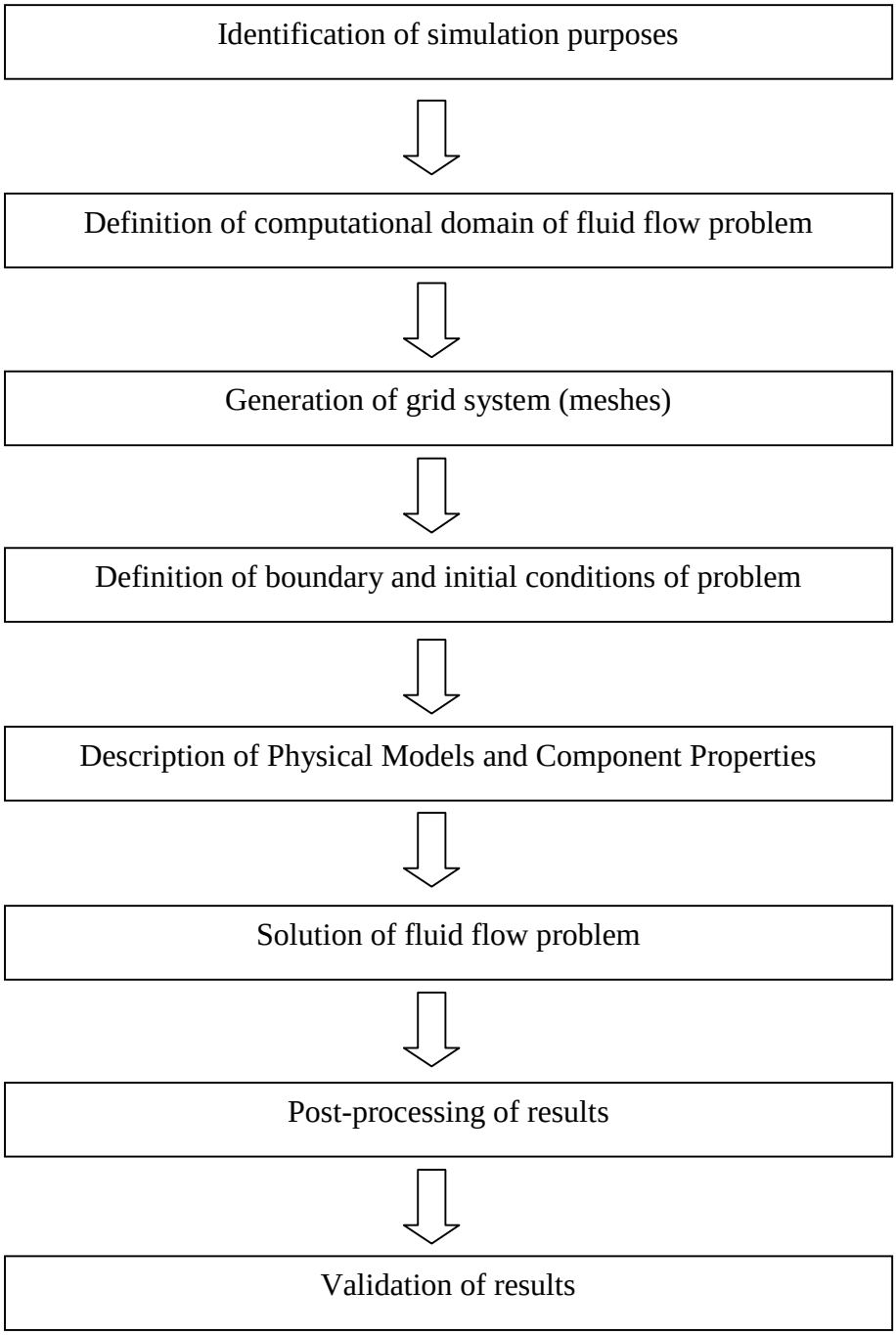

3.2 Introduction to Flow 3D

In this thesis, Flow 3D is used in the solver step. It provides a powerful tool for complex fluid modeling problems. Flow 3D enables highly accurate simulations of free-surface flows using TruVOF, a modified version form of the Volume of Fluid technique (www.flow3d.com). Flow 3D solves the Navier-Stokes in three dimensions to simulate the fluid flow equations together with the continuity equations and some advection equations for the turbulence quantities for turbulence closure.

Flow 3D uses the finite-volume method to solve the RANS equations. A rectangular grid of cells (meshes) is formed subdividing the computational domain. Rectangular grids are very easy to generate due to the regular nature of rectangular mesh system. After the computational domain is subdivided by meshes, the solution is performed based on a unit cell. The computational cells are identified in x-direction (i), y-direction (j) and z-direction (k). Scalar quantities are calculated at the cell centers whereas vector and tensors are calculated at the cell faces. The grid system for Flow 3D is shown Figure 3.1.

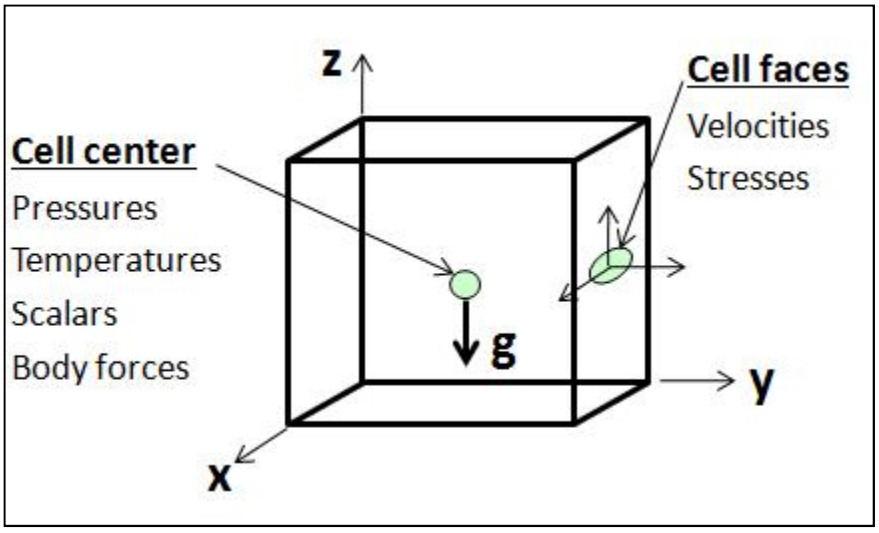

Figure 3.1 Grid System for Flow 3D (Flow 3D Advanced Hydraulic Training-2012)

Flow 3D includes many optional physical models that are added to or modified the basic Navier-Stokes equations. These additional items are describing the effects of turbulence, surface tension, heat transfer, fluid solidification, sediment scour, Lagrangian particles, granular flows, moving solids, solid deformation, air entrainment, cavitation, and porous media.

Flow 3D could be worked in different modes such as compressible flow, incompressible flow situations or limited compressibility conditions. Furthermore, there are one fluid or two fluid models in Flow 3D. In this thesis, the one-fluid incompressible mode is used while modeling the free surface. General solution method for an incompressible flow of Flow 3D is shown Figure 3.2.

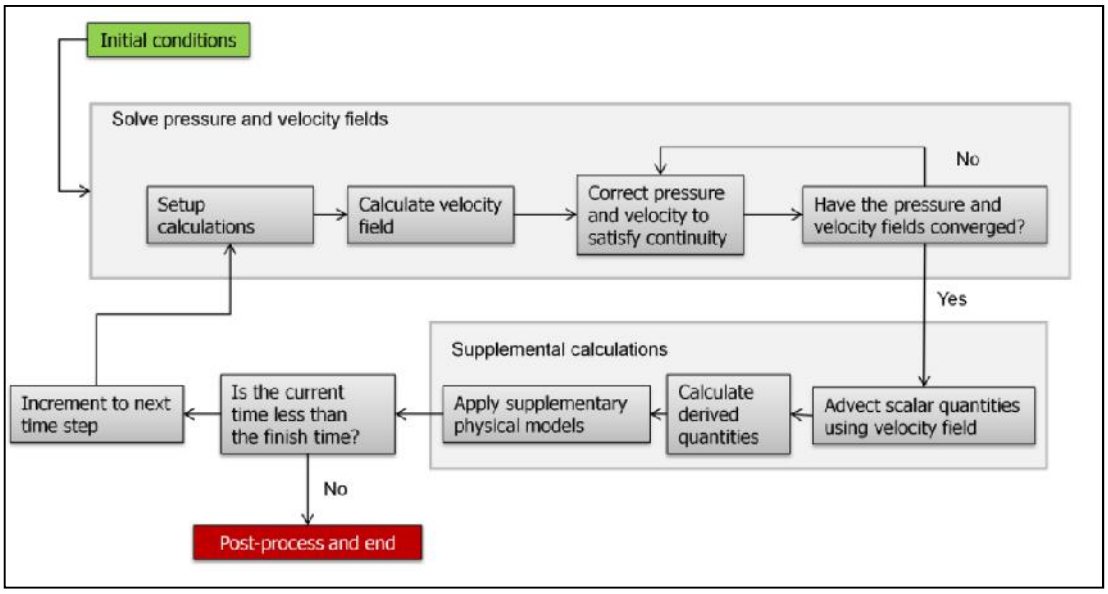

Figure 3.2 General Solution Method for an Incompressible Flow (Flow 3D General Training Class-2013)

3.2.1 Discretization Techniques

The three dimensional flow field is governed by the continuity and the momentum equations. Navier-Stokes equations are the most general description of a fluid flow. If the density of the fluid may be considered as constant, the Navier-Stokes equations

simplify for incompressible fluids. A fluid element can be thought of as the smallest volume for which the continuum assumption is valid. That is, computational domain is represented by many small control volumes.

A computational mesh should effectively discretizes the physical space. During the process of integration, it is presumed that the cell is small enough that the flow parameters do not vary crucially at this scale. The free surface is computed using TruVOF. The control volume representation of Flow 3D is shown in Figure 3.3.

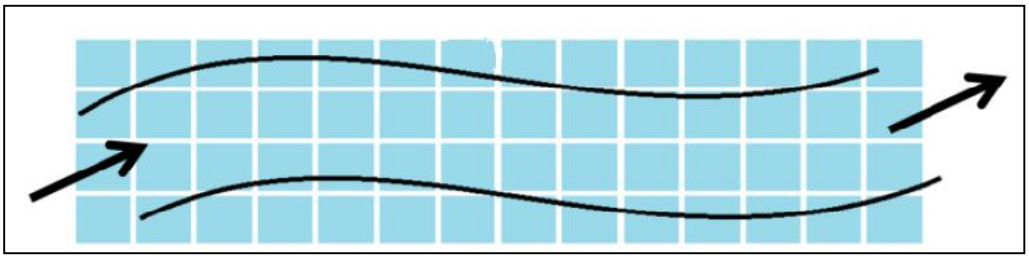

Figure 3.3 Control Volume Representation in Flow 3D (Flow 3D General Training Class-2013)

The VOF method was improved by Dr. Tony Hirt. The VOF method obtains an accurate way to advect fluid interfaces through a computational grid while keeping the interface sharp and well defined. Hirt and Sicilian (1985) represented the Fractional Area/Volume Obstacle Representation (FAVOR) method. FAVOR method uses the similar approach of VOF free surface definition while defining the obstacles.

The geometry of the problem in the computational domain subdivided the rectangular grids are defined using the FAVOR method. The control volumes in Flow 3D are defined as rectangular bricks. Each cell is arbitrary geometry and flow areas. FAVOR method is similar to the VOF method in defining cells that are empty, full, or partially filled with fluid.

For a one fluid mode in Flow 3D, F represents the volume fraction occupied by the fluid so that fluid exists where F equals to 1. On the other hand, absence of fluid or void regions corresponds to locations where F equals to 0.

The FAVOR concept can be used in connection with any type of grid including grids consisting of rectangular or distorted elements and whether the grid is structured or unstructured. Structured grids are best because they are easy to generate and the indices for neighboring elements are known. Rectangular grid elements make it easy to compute the fractional areas and volumes of elements used by the FAVOR method (www.flow3d.com). Additional to the FAVOR method, free gridding approach which is consisted with simple rectangular mesh elements and multi-block meshing option increases program capability compared with other CFD softwares. In free gridding approach the geometry building does not depend on the gird generation. Both of operations are completed separately. A VOF method must include an algorithm for following the sharp interface between the fluid and void. The representation of sharp interface of fluid fraction in Flow 3D is shown in Figure 3.4. The TruVOF is Flow 3D's VOF advection technique. TruVOF provides these capabilities and includes enhancements to maintain the sharp interface.

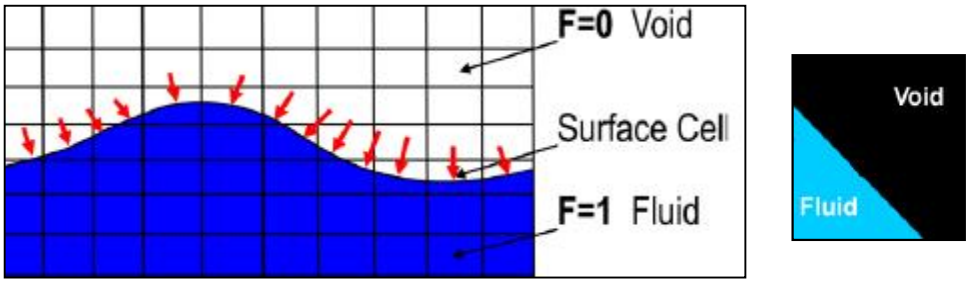

Figure 3.4 Sharp Interface of Fluid Fraction (Flow 3D Advanced Hydraulics Training-2013)

In order to model a free surface, it is significant that the free surface must be accurately tracked. Firstly, there must be a fluid fraction variable F, which accurately locate and orient the free surface. The grid porosity value is zero within full obstacles

and no fluid whereas the value of grid porosity is 1 for cells within full fluid and no obstacles. On the other hand, cells only partially filled within obstacle have a value between zero and 1, based on the percent volume that is solid. Secondly, an advection algorithm is necessary to define surface as a sharp interface between the fluid and air. Third, free surface boundary conditions must be applied to the interface. FAVOR concept calculates the area and volume ratios in each staggered cell and the ratios are integrated into conservation equations (Figure 3.5).

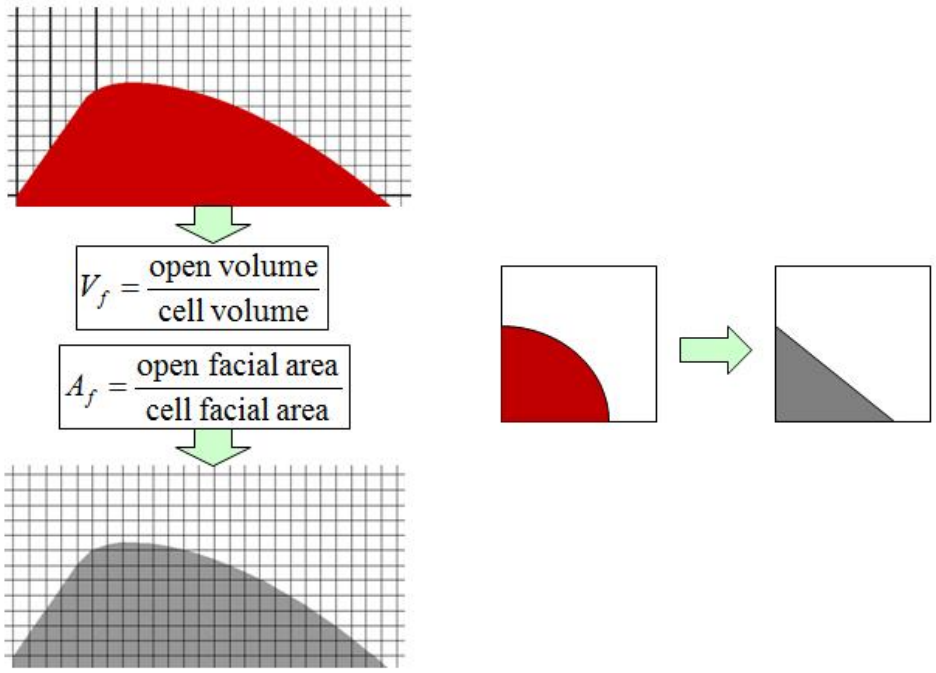

Figure 3.5 FAVOR (Introduction to Flow 3D for Hydraulics-2013)

The most important advantage of the FAVOR technique is that a grid system is independent of the domain geometry. That is, the variations of geometry such as adding or modifying geometry of the numerical model do not affect the grid generation.

CHAPTER 4

NUMERICAL MODEL IMPLEMENTATION

4.1 Pre-Processor

Pre-Processor can be separated into following components: geometric representation, grid generation, definition of boundary and initial conditions. In addition, it is necessary to identify the physics, primarily related to the fluid properties.

4.1.1 Geometric Representation

Three-dimensional solid geometry of Laleli dam spillways is drawn using AutoCAD-3D Modeling tool. Both the three dimensional solid drawings of physical model geometry and prototype geometry are prepared. In the physical model of Laleli dam spillway, a unit channel is placed in the middle and two half channels are symmetrically placed on both sides of the unit channel to avoid sidewalls effects. Then, the drawings of Laleli dam spillway are exported as the stereo lithographic (.stl) file format which could be read by Flow 3D from AutoCAD. The geometric representation of Laleli dam spillway model is shown in the Figure 4.1.

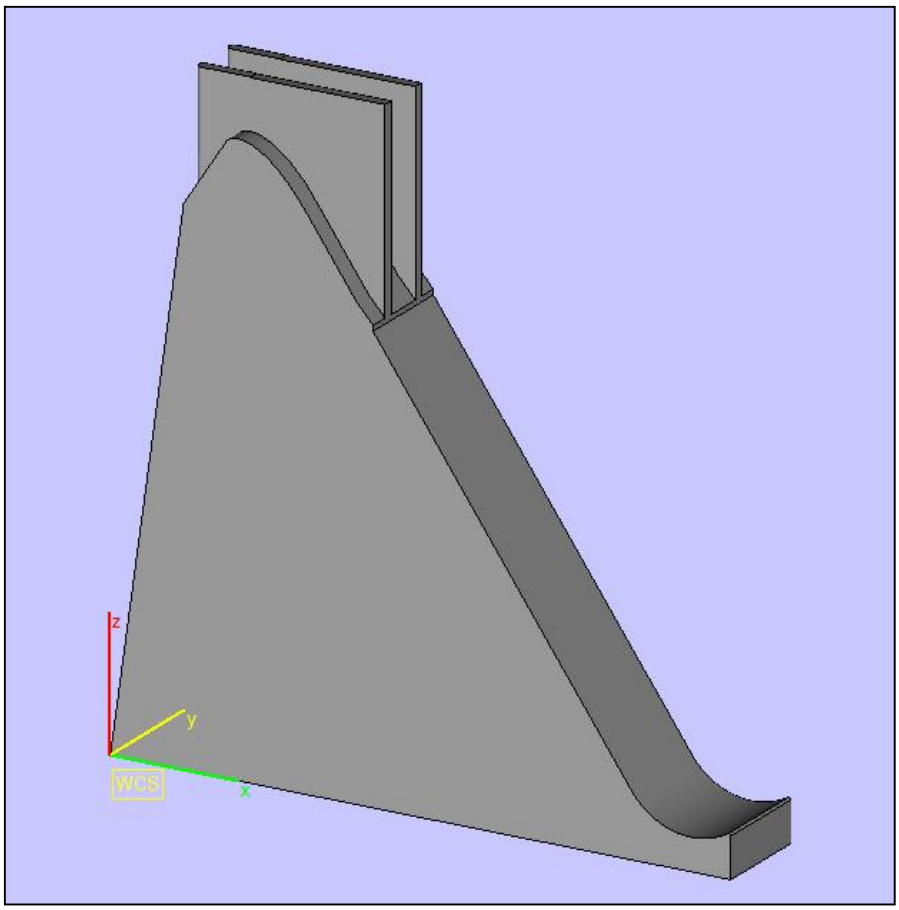

Figure 4.1 Physical Model Geometry of Laleli Dam Spillway (TR-5)

The solid object surface is identified by triangles in .stl format and the .stl object must be a closed surface. There can be some errors in the .stl geometry files generated by AutoCAD or other 3D modeling software. The errors in .stl geometry files cannot be seen in the Flow 3D Meshing and Geometry view tab and this situation may affect the solution accuracy. Thus, all .stl files should be controlled for accuracy before they are imported into Flow 3D. MiniMagics is a free tool software that is provided with Flow 3D to check and correct the .stl files. All most of geometry files can be controlled by using this software.

After the .stl file is imported into Flow 3D, the geometry of spillway is embedded in the computational grid by the pre-processor using the FAVOR concept.

4.1.2 Grid Generation

In Flow 3D, grid generation is the most important issue for accurate solution. If good quality of mesh is generated, one can obtain realistic results from the numerical model. The first step in identifying a computational domain of the fluid flow problem is to determine the type of coordinate system to use for the mesh. Flow 3D uses a grid system of orthogonal meshes in the Cartesian or cylindrical coordinates. All mesh blocks in the numerical model are generated by the coordinate system which is selected by the user. Cartesian coordinate system is selected for this investigation. The flow region is subdivided into a mesh of fixed rectangular cells. The grid generation does not depend on the geometry. That is, the geometry in the domain is represented in a simple and proper way without requiring a body fitted grid system so that the geometry and grid generation are independent of each other.

Mesh size should be determined carefully to obtain accurate results. Definition of the grid spacing is a significant aspect of the model development especially close to the solid walls. A considerable amount of grid refinement should be made to resolve the boundary layers. However, for an inclined surface over which there is a high velocity flow at a very small depth like in the flow over Laleli dam spillway it is not possible to maintain a refined grid close to the spillway chute. This can only be maintained with a very fine grid all over the flow domain which results with a huge mesh that cannot be run. Hence, in this thesis, two grid systems are tried. Firstly, the geometry is in the Cartesian coordinates (Case 1). Secondly, the flow direction is in the Cartesian coordinate by rotating the spillway 55° about y-axis so that that the primary flow direction is in one of the Cartesian mesh directions that allowed a mesh refinement only close to the spillway chute (Case 2).

In Case 1, the geometry of Laleli dam spillway is placed on the Cartesian coordinates (Figure 4.2). The computational domain has to cover the fluid flow, but its size should be minimized for an economical solution.

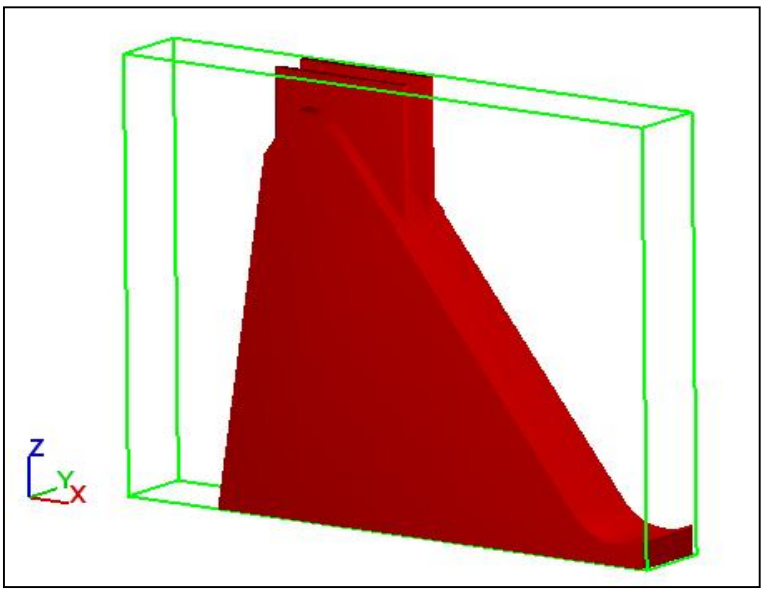

Figure 4.2 Computational Domain of Case 1

The definition of mesh size is another part of implementing the numerical model. It affects the accuracy of the simulation directly. For Case 1, a uniform mesh is used in all three Cartesian coordinates (Figure 4.3).

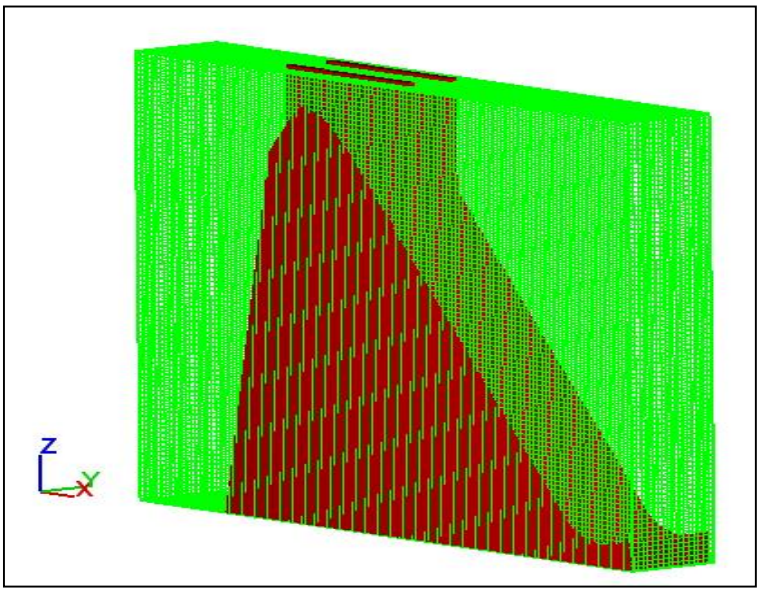

Figure 4.3 Grid Generation of Case 1

As a second trial, to decrease the total mesh size and impose the desired grid spacing close to the spillway chute, the spillway geometry is rotated 55° about the y-axis so that primary flow direction is in the Cartesian mesh coordinate x-direction. The computational domain of Case 2 is shown in Figure 4.4.

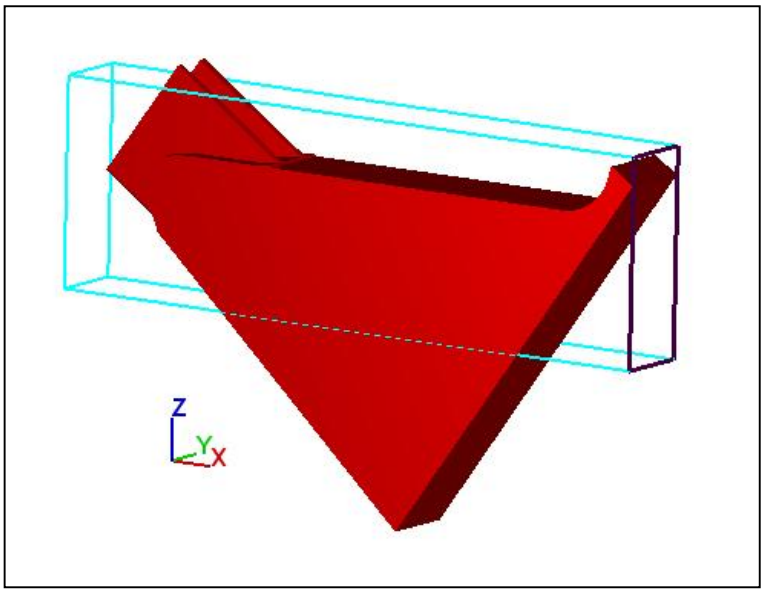

Figure 4.4 Computational Domain of Case 2

Computational domain of Case 2 is smaller than Case 1. Moreover a grid refinement is done close to the spillway chute. This situation provided a much faster solution for Case 2. (Figure 4.5)

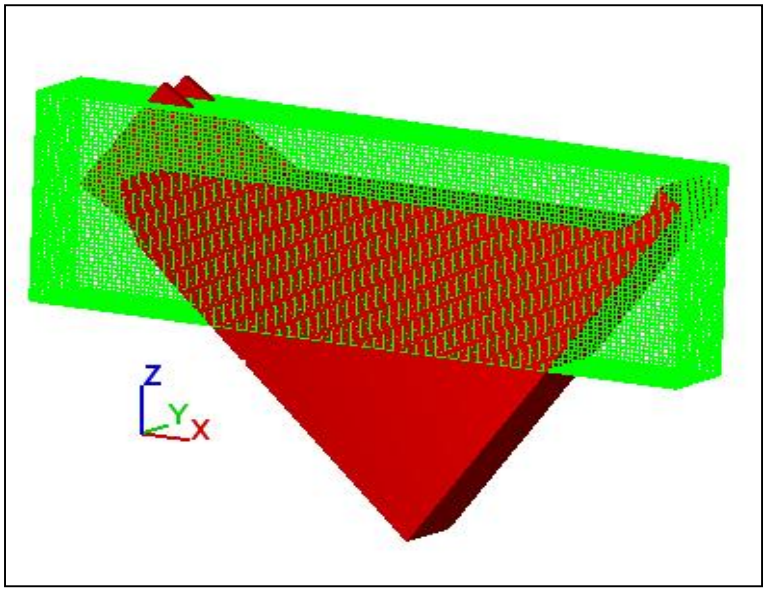

Figure 4.5 Grid Generation of Case 2

For Case 2, a uniform mesh is used for the first of four simulations. Furthermore, non-uniform mesh system is generated adding mesh planes along the chute surface for other trials in order to provide more grid refinement close to the spillway chute. For non-uniform mesh system, there are some advices in Flow 3D Users Manuel in order to generate an appropriate grid. The most significant issue is to avoid large differences in sizes between adjacent cells. The size ratio between adjacent cells should be as close to unity as possible, and not exceed 1.25 for efficient results. Also, cell aspect ratios should be as close to unity as possible, and not exceed 3.0 because cell aspect ratios which are exceeded 3.0 cause pressure iteration difficulties. (Figure 4.6)

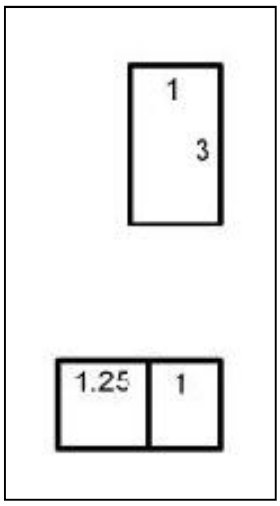

Figure 4.6 Cell Aspect Ratio and Size Ratio (Flow 3D Lecture Notes)

Figure 4.7 shows the numerical model with additional mesh plane in order to provide more mesh refinement at spillway surface.

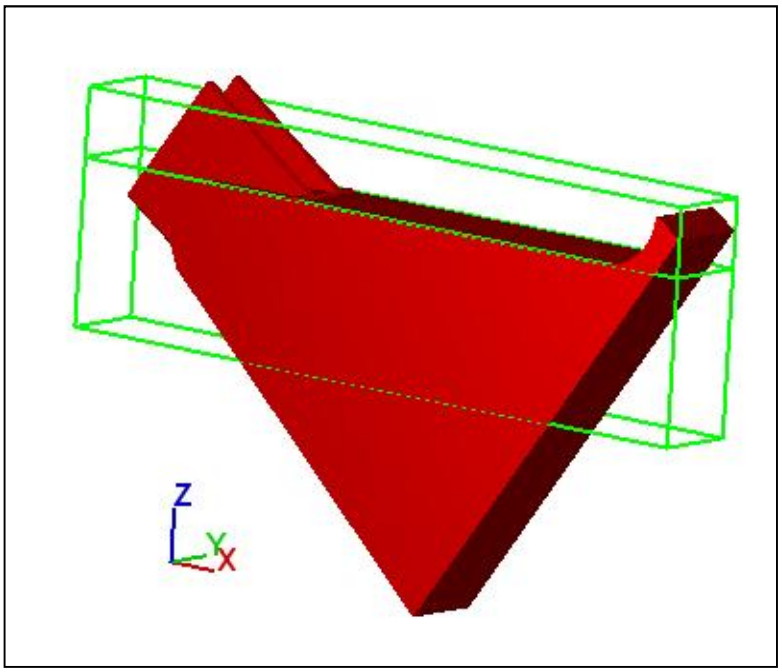

Figure 4.7 Non-Uniform Grid Generation with 2 Mesh Planes

4.1.3 Boundary and Initial Conditions

Determination of the appropriate boundary conditions is one of the most important phases of the numerical flow analysis. The boundary conditions must be matched with the physical conditions of the problem properly. Flow 3D uses the orthogonal hexahedral meshes in the Cartesian coordinates in order to define the three dimensional flow domain. Thus, there are six different boundaries which are defined on rectangular mesh prism.

For the numerical analysis which consist reservoirs of fluid, pressure boundary condition is represented. There are two types of pressure boundary conditions in Flow 3D. These are described as static or stagnation pressure conditions. In a static condition, the pressure is more or less continuous across the boundary and the velocity at the boundary is assigned a value based on a zero normal-derivative condition across the boundary. In contrast, a stagnation pressure condition assumes stagnation conditions outside the boundary so that the velocity upstream from the boundary is zero. This assumption requires a pressure drop across the boundary for flow to enter the computational region. (Flow 3D-User Manual)

For free surface and incompressible fluid flows, the outflow boundary condition could be used for exit condition. In symmetry boundary condition, no shear stresses are calculated across the boundary. Wall boundary condition is used for side of the spillway model to represent the physical model environment. The boundary conditions used by this study are below.

Upstream boundary: Stagnation pressure condition (Hydrostatic pressure with zero velocity)

Downstream boundary: An outflow condition

Top boundary: Symmetry condition (Inactive Boundary)

Bottom boundary: Wall condition (Inactive Boundary)

Side boundary: Wall condition (Smooth Wall)

For initial condition, a fluid region is defined inside the reservoir and located at the crest of the spillway. Flow velocity is set to zero due to the condition of stagnation pressure.

The Favorized geometry of Laleli dam spillway is on the Figure 4.8 for Case 1. It is shown with fluid region as reservoir.

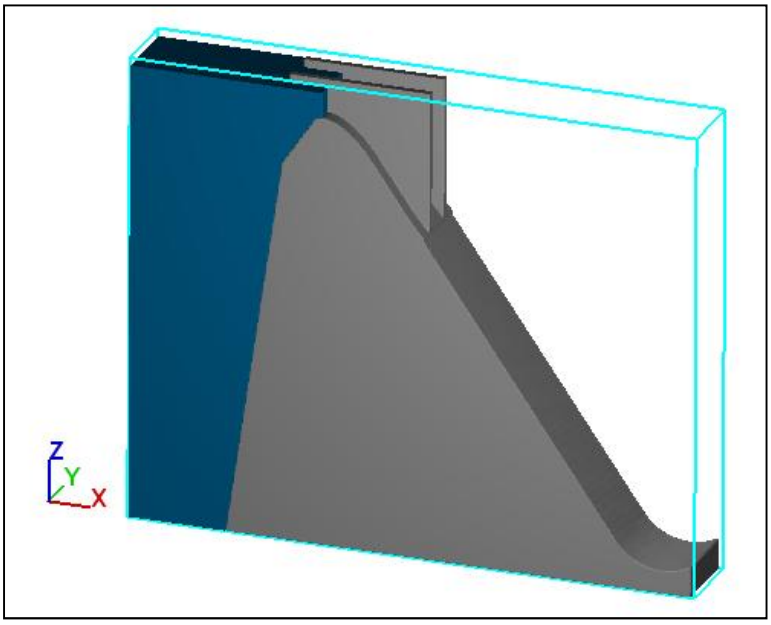

Figure 4.8 Initial Condition of Case 1

The geometry of spillway is rotated 55° for Case 2 so that the boundary conditions must be set with respect to this situation. The fluid region must be also rotated 55°. Furthermore, in order to use stagnation pressure condition, initial fluid height must be updated with respect to Cartesian coordinates (Figure 4.9).

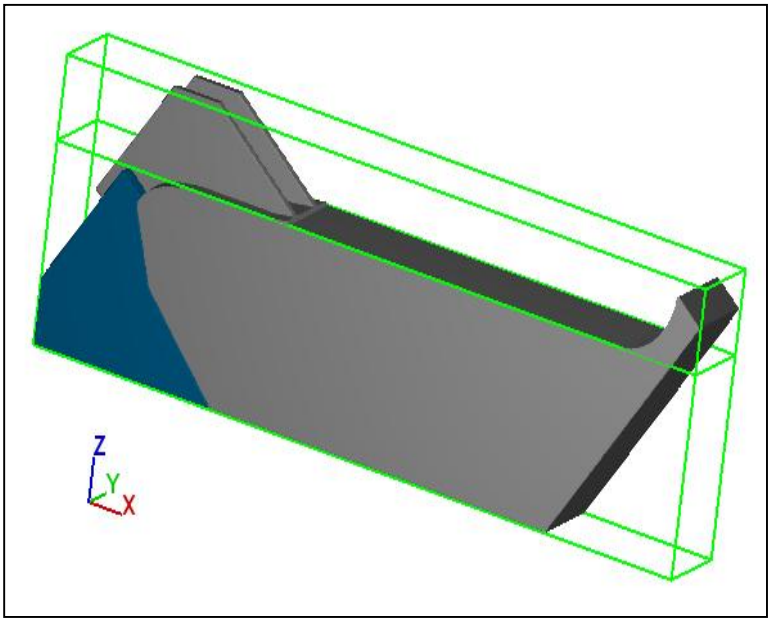

Figure 4.9 Initial Condition of Case 2

4.1.4 Physics

Physical models in Flow 3D can be separated into two parts. These are subgrid models and supplementary models. Subgrid models are semi-empirical models and they have an adjustable parameter for calibration such as the air entrainment model. On the other hand, supplementary models are analytical.

"Viscosity and turbulence", "gravity and non-inertial frame" and "air-entrainment" options are activated in the physics tab during this study.

4.1.4.1 Turbulence Modeling

There are five turbulence models available in Flow 3D. These are the Prandtl mixing length model, the one-equation, the two equation k - ε and RNG models, and a large eddy simulation (LES) model. In this thesis, Renormalization group turbulence model is selected.

RNG model solves the same equations with the k - ε model. However, constants of turbulence equations that are found empirically in the standard k – ε model are derived explicitly in the RNG model. Generally, the RNG model has wider applicability than the standard k - ε model. In particular, the RNG model is known to describe low intensity turbulence flows and flows having strong shear regions more accurately (Flow 3D User Manuel). Turbulence models can be selected and activated in Physics tab, Viscosity and Turbulence option.

4.1.4.2 Air Entrainment Model

Air entrainment model is used to the approximate the aeration of fluid flow. This model does not require two phase solution. The air entrainment model is activated in Physics tab, Air entrainment option. The entrainment rate coefficient is selected as 0.5. It must be a positive value and the default value in Flow 3D is 0.5 and this value which is suitable for most cases is recommended by Flow 3D User Manuel. Surface tension coefficient is also selected the default value of 0.073. The bulking option is also activated in order to see effect of the entrained air on the fluid density. Volume fraction of entrained air is calculated when this model is activated. Air has a density of approximately 1.225 kg/m^3 so that density of phase #2 is selected as 1.225.

4.1.4.3 Gravity

Gravity vector components are defined using Physics tab in Gravity and non-inertial reference frame option. Activate Gravity is selected and the components of the gravity vector in the Cartesian coordinates are entered. The gravity vector direction is constant during the simulation.

Gravity has an approximate value of 9.81 m/s^2. In Case 1, gravity is entered in negative z-direction, g_z = -9.81 m/s^2 (Figure 4.10). In Case 2, gravity components are entered as g_x = 9.81 * sin55 = 8.035 m/s^2, g_y = 0 and g_z = 9.81 * cos55 = -5.627 m/s^2. (Figure 4.11)

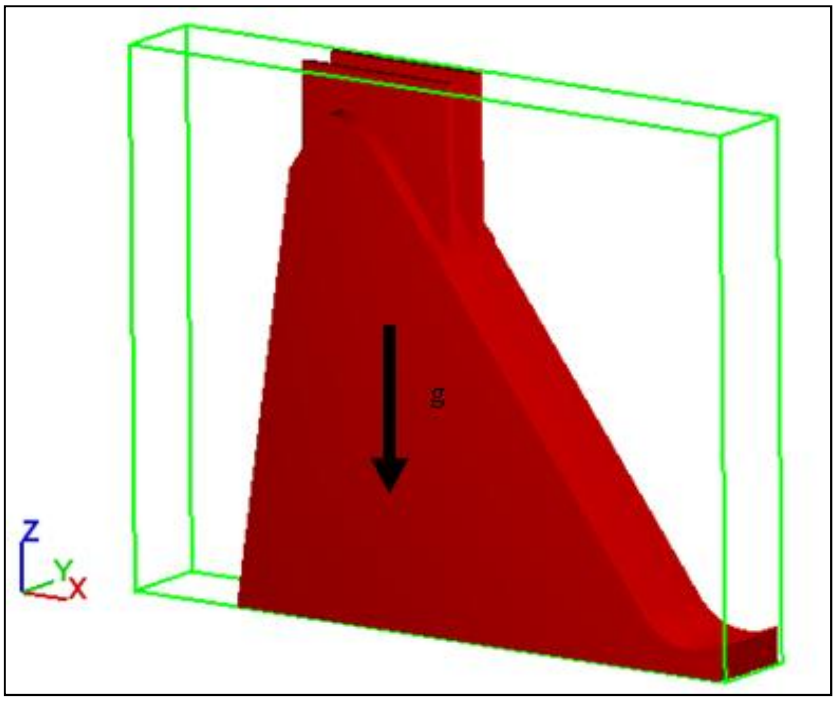

Figure 4.10 Gravity Vector For Case 1

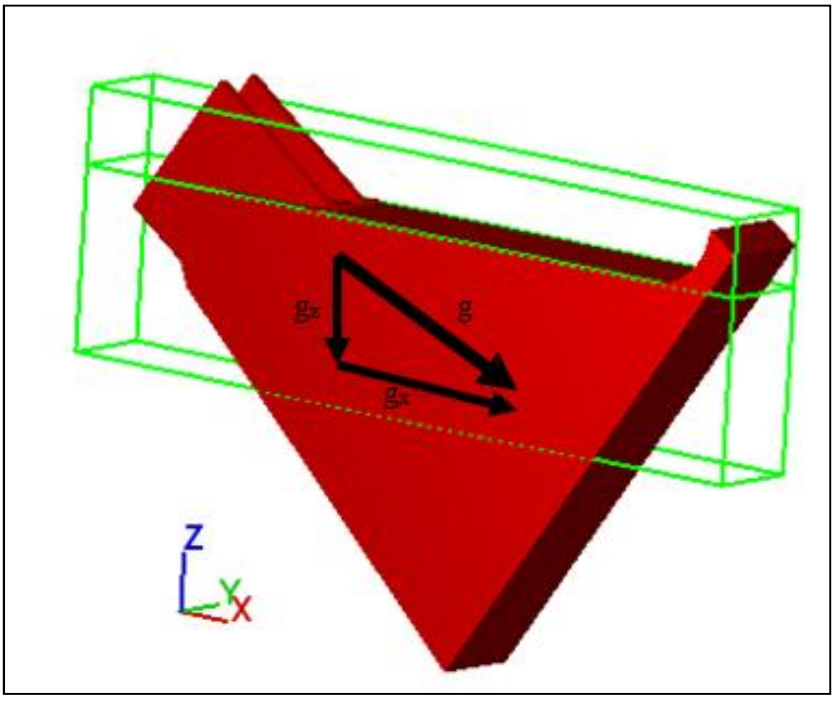

Figure 4.11 Gravity Vector For Case 2

4.1.5 Material Properties

Fluid properties such as density, viscosity and temperature must be defined as an input for the numerical model. Fluid is selected using fluid database tab and fluid properties are specified on the Fluids tab. In Flow 3D, there is a library of common materials to aid the user. Solid properties are defined per component using Meshing and Geometry tab. During this study, Water at 20 °C is chosen.

4.2 Solver Options

There are many parameters affecting the simulation results and time. Solution method (implicit or explicit), time step size, convergence settings and numerical approximations are some of them. Balancing run time and accuracy of simulation is a significant point. In order to provide optimum and efficient solution of a simulation, choosing the appropriate numerical options is very important. Numerical options are specified in the Numerics tab. In this thesis, the water is used in all simulation. It is assumed to be incompressible and only one fluid is solved in all of the simulations. Pressure solver is selected as implicit since pressure forces in the momentum equation are always approximated implicitly for incompressible fluids as a means of maintaining the incompressibility of the fluid and stability of the solution. (Flow 3D-User Manuel)

In Numeric option, GMRES algorithm is the default iteration method and this method can be used for a wide range of problems. It is recommended by Flow 3D for all kinds of flow problems. While computing the viscous stresses, explicit viscous algorithm is used.

There are many options in Flow 3D to track fluid interfaces. Automatic option is used as volume of fluid advection model to track fluid interface. For a sharp interface with one fluid free surface flows, the automatic option is the most efficient and accurate model in Flow 3D.

First order momentum advection is selected due to the fact that it is robust and sufficiently accurate for the spillway flow.

CHAPTER 5

NUMERICAL SIMULATIONS RESULTS

Numerical simulations are evaluated and results of the simulations are compared with each other and the physical model results in this chapter. In the hydraulic model, the similarity was achieved by the Froude similarity law. The model scale of 1:25 was selected in the physical tests. Table 5.1 summarizes the scaling ratios for the Froude similitude, where length ratio $l_r = 25$.

Table 5.1 Scaling Ratios for Froude Similitude

Parameter	Unit	Scale Ratio with Froude Law	Value of Scale Ratio
Length	m	l_r	25
Area	m^2	l_r^2	625
Velocity	m / s	$l_r^{0.5}$	5
Discharge	m^3 / s	$l_r^{2.5}$	3,125
Pressure	Pa	l_r	25

Flow analysis of Laleli dam spillway consists of the following topics: Grid selection and mesh refinement, air entrainment and scale effects and investigation of cavitation potential.

The test case has the following flow conditions. The inlet discharge is specified at a 1000 years return period flood discharge (Q_{1000}). The height of the physical model of Laleli dam spillway is 4.46 meters, with a design head of $H_0 = 0.26$ m.

Simulations are continued until convergence of various flow parameters with respect to steady state condition is obtained. Several simulation scenarios are implemented using the operation conditions of the physical model and prototype.

5.1 Grid Selection and Mesh Refinement

Grid selection is one of the most important challenges of this thesis. Flow 3D uses a non-body fitted structured orthogonal mesh in the Cartesian coordinates which does not depended on the geometry. Due to the geometry of Laleli dam spillway, obtaining the required mesh resolution is a hard process. In the stage of grid selection, Case 1 and Case 2 are investigated as described in Chapter 4. The simulations for appropriate grid selection are focused on physical model test case, scenario TR-5.

In Case 1, the flow direction over the spillway is not in one of the Cartesian coordinates. Hence, it is not possible to make locally the necessary mesh refinement close to the spillway surface. Therefore, in Case 2, the geometry of Laleli dam spillway is rotated 55° so the flow over the spillway is coincident with one of the Cartesian coordinates. Initially, a coarser mesh is used for quick convergence for both of these cases. After convergence is reached using coarser mesh, the mesh size is gradually reduced. During the mesh refinement process, favorized geometry and mesh can be controlled by Favorize option in the model setup. The favorize option gives an idea about appropriate discretization of the geometry.

Mesh independency of the numerical results is one of the main issues of an accurate simulation so that mesh refinement process should be completed before starting and evaluating a numerical study. Moreover, while an accurate solution is sought, an efficient and optimum solution with regards to runtime is also required. Although generally finer meshes give more reliable results, limitations in computer memory and runtime restrict the number of grid points that will be used in a simulation.

In order to verify the applicability, numerical model results are compared with the physical model of Laleli dam spillway. The physical model tests were performed by Aydın et al. (2012) based on a Froude similitude model of the spillway of 1:25 scale. The pressure values along the spillway crest and chute for different numerical model simulations are compared with the results which were measured from the physical model. In the physical model tests, the piezometer heads were measured at 53 points over the spillway central axis. These points over the spillway are shown in Figure 5.1.

In the physical model study, the measurements are especially done beginning from the 22nd point because the risk of cavitation starts after this section. There are no measurements at points 28, 29 and 30 along the spillway surface due to the fact that the aeration ramp is located there. Pressure values at the same points are extracted from the numerical solutions and compared with the experimental results. The pressure head values along the measurement points over the spillway for different mesh sizes are represented.

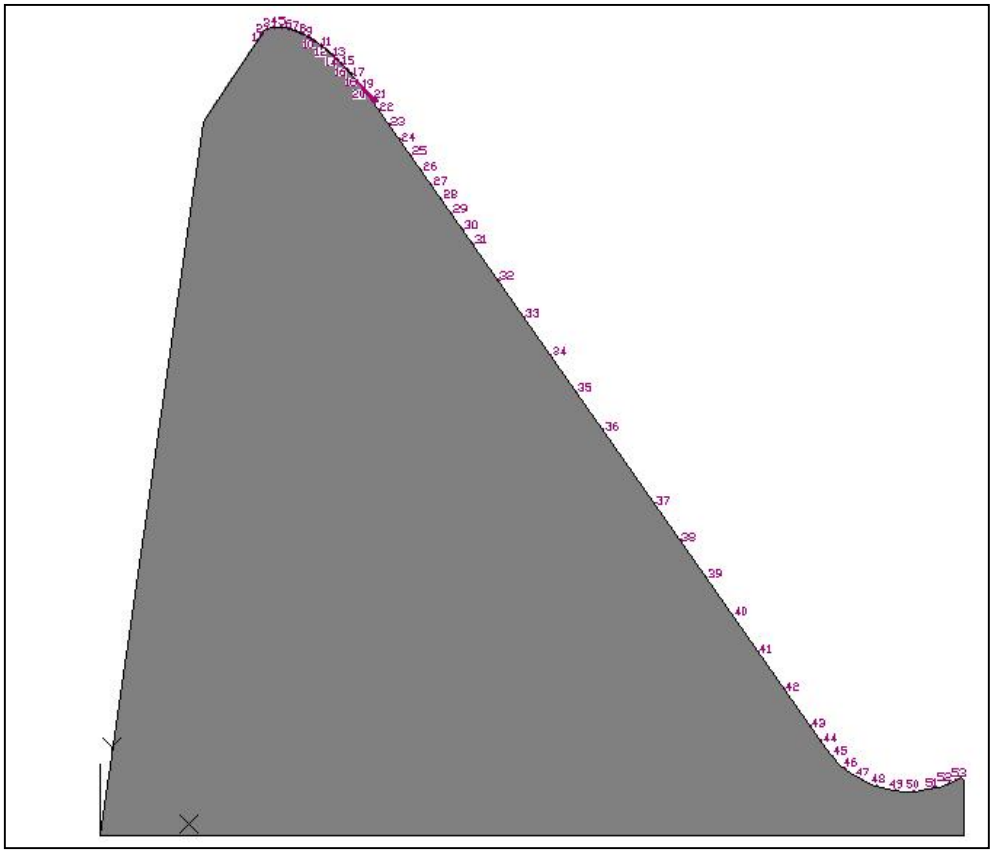

Figure 5.1 Measurement Points over the Physical Model

5.1.1 Simulations for Case 1

For Case 1, geometry of Laleli dam spillway is arranged so that gravitational acceleration is on the –z Cartesian coordinate. Five simulations are done from coarser mesh to finer mesh in order to obtain grid independency. A uniform mesh is used in all simulations for Case 1, meaning that the identified cell size is the same in all three Coordinate directions. Cell size and the total number of grid points for different simulations for Case 1 are given in Table 5.2.

Table 5.2 Summary of Grid Generation Trials for Case 1

Simulation #	Cell Size (m)	Total Number of Cells
NM 1	0.050	178,176
NM 2	0.035	523,066
NM 3	0.020	2,784,000
NM 4	0.015	6,563,520
NM 5	0.010	22,272,000

As it can be seen from Table 5.2 reducing the mesh size in all over the domain considerably increases the total number of grid points.

Initial simulation is completed with a 0.050 m mesh size and using Flow 3D's add restart simulation option, mesh size is gradually decreased to improve accuracy obtaining good initial condition from the former simulation. The last simulation is NM 5 for Case 1 where a mesh size of 0.010 m is used. Total number of grid points for this simulation is 22,272,000. Another simulation with a finer mesh was not run as the computational time would be much longer.

Volume flow rates for all simulations are given in Table 5.3.

Table 5.3 Volume of Flow Rates for Case 1

Simulation #	Volume Flow Rate in Model (l/s)	Relative Error (%)
NM 1	181	8.4
NM 2	177	6
NM 3	182	9
NM 4	183	9.6
NM 5	178	6.6
Experiment	167	-

As it can be seen from Table 5.3, the volume flow rates are close to each other and these values show a good agreement. Numerical model results for discharge values are slightly larger than the experimental value but it is an acceptable difference. Pressure head values obtained at the measurement points are compared for the experimental and numerical results with different mesh sizes in Figures 5.2 - 5.6.

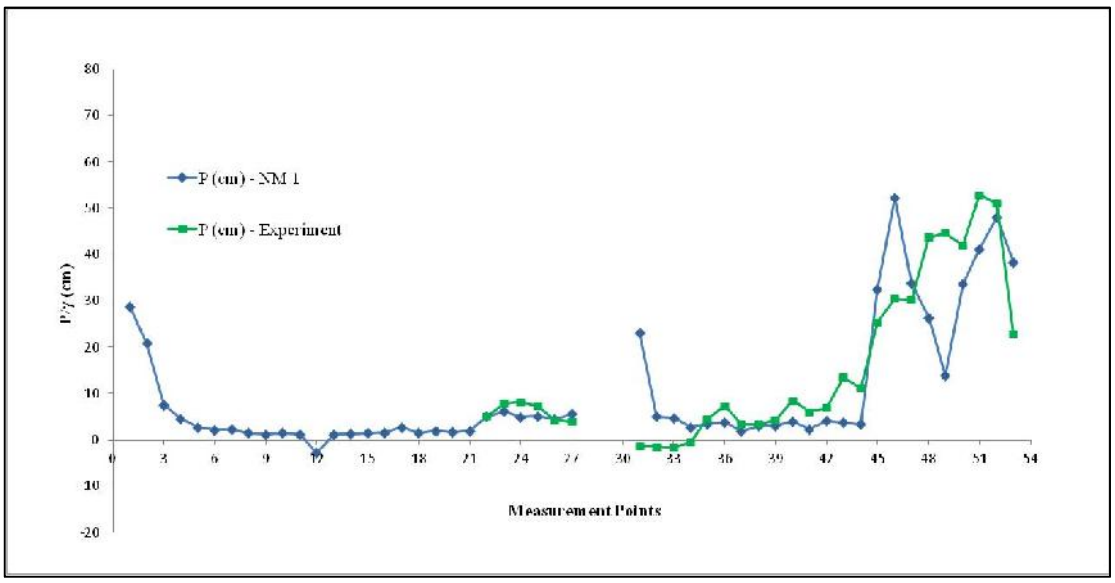

Figure 5.2 Comparison of Pressure Head Values Along The Measurement Points for NM 1 and Experiment

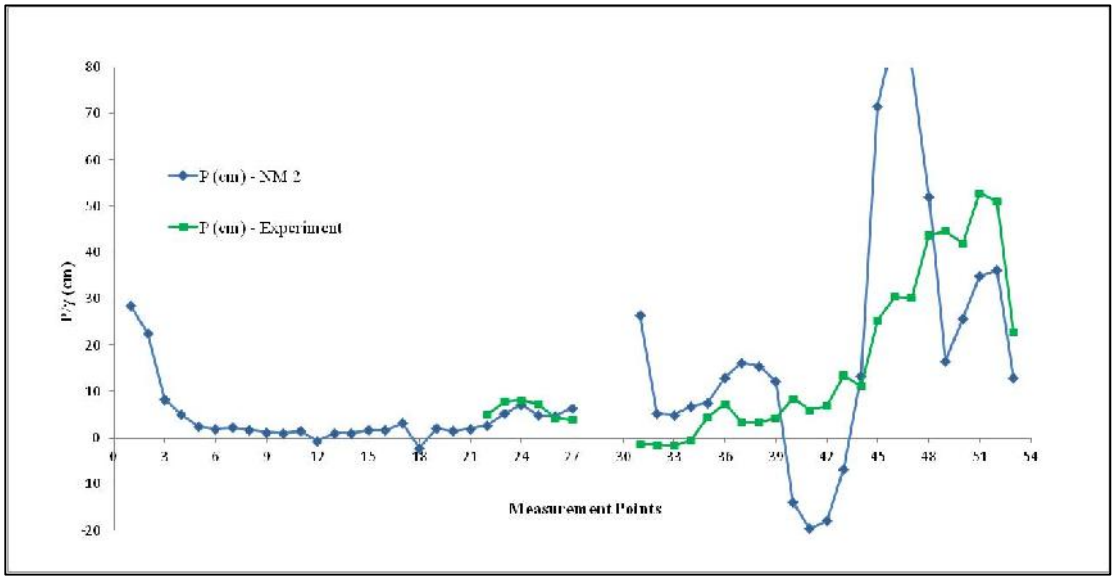

Figure 5.3 Comparison of Pressure Head Values Along The Measurement Points for NM 2 and Experiment

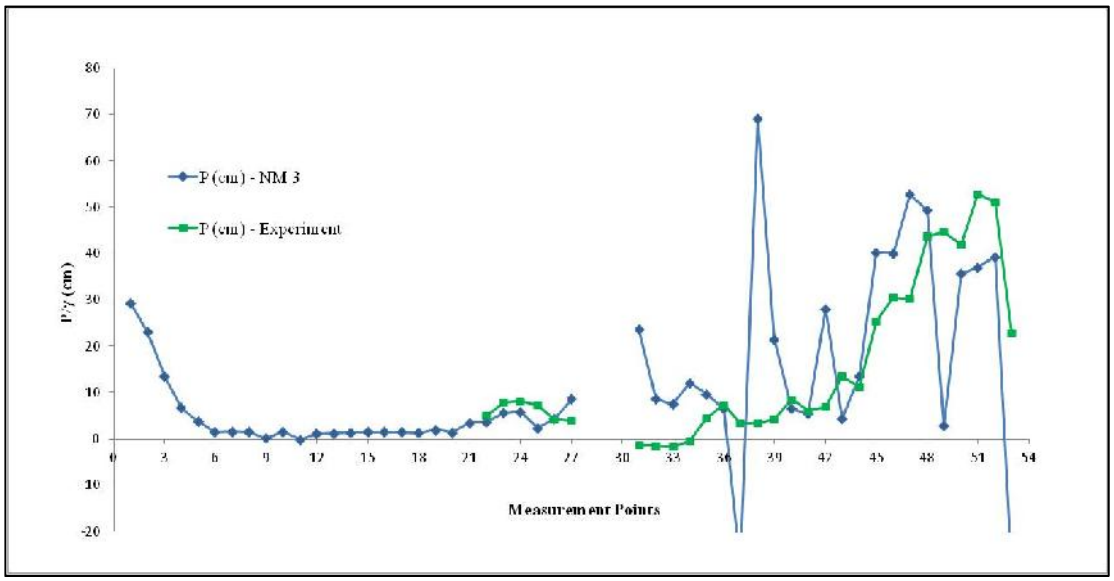

Figure 5.4 Comparison of Pressure Head Values Along The Measurement Points for NM 3 and Experiment

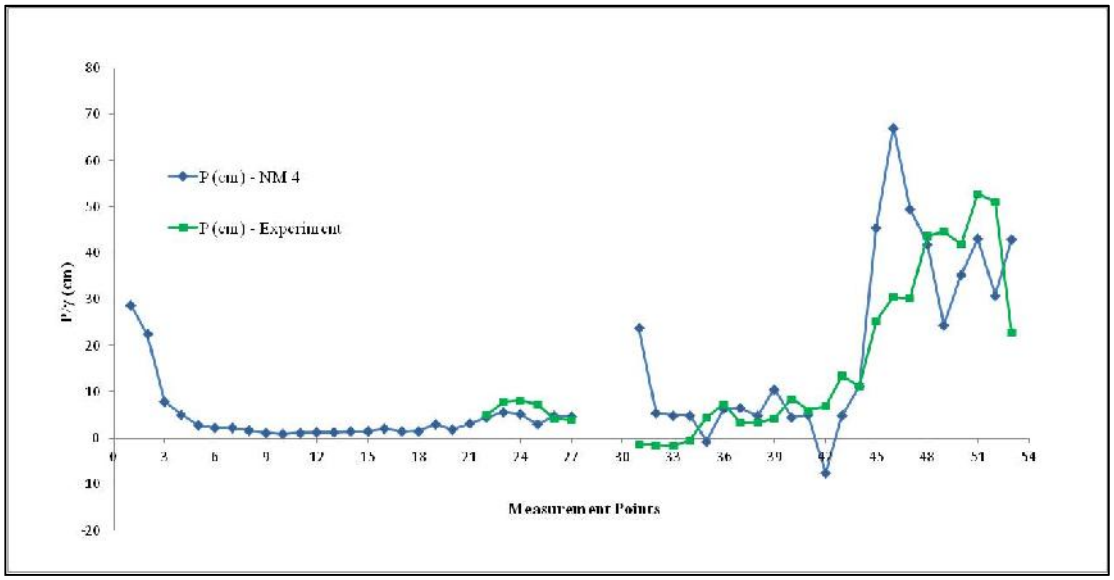

Figure 5.5 Comparison of Pressure Head Values Along The Measurement Points for NM 4 and Experiment

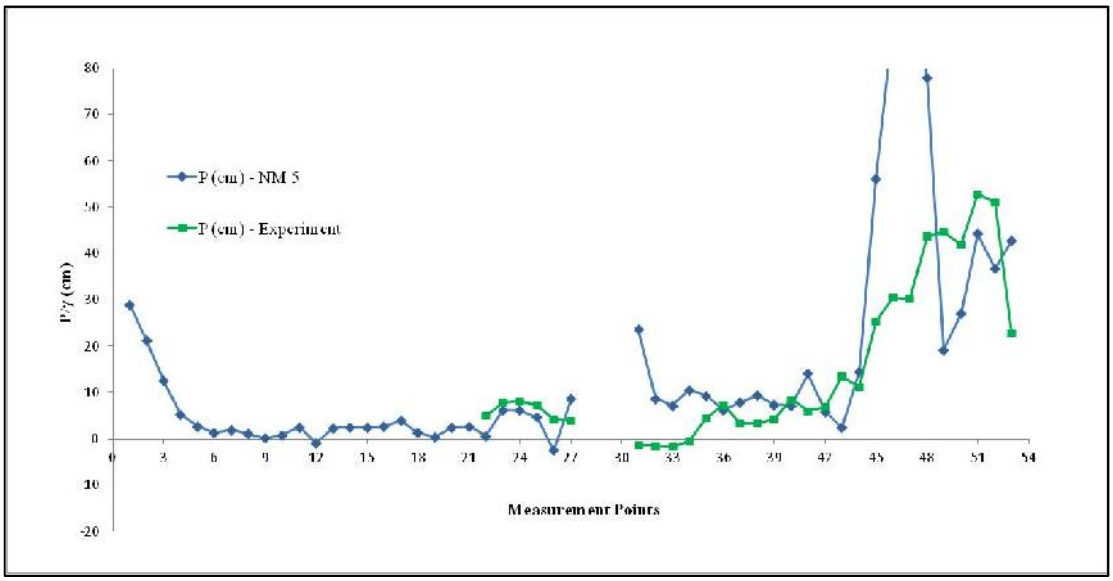

Figure 5.6 Comparison of Pressure Head Values Along The Measurement Points for NM 5 and Experiment

In overall as the mesh size decreases a better agreement between the numerical and experimental results is achieved. Although the pressure head values matched well with the experimental data before the aeration ramp for all the mesh sizes, the pressure trend is not compatible with the physical model results especially after the aeration ramp for large mesh sizes. In NM 5, even a reasonable agreement on the pressure values over the flip bucket, which is the most problematic part in terms of the agreement with the experiment, is achieved.

Despite of the good estimation on volume flow rates for all mesh sizes used in Case 1, there are some problems in the pressure head estimations in the simulations. For example pressure head value at point 31 is over estimated in all the simulations with different mesh sizes. Although a fine mesh size is used to resolve the geometry flow over the spillway is not accurately solved. This is because of the insufficient number of grid points along the flow depth.

5.1.2 Simulations for Case 2

For Case 2, geometry of Laleli dam spillway is rotated 55° so that flow over the spillway is coincident with one of the direction of Cartesian coordinates. By doing this more grid points are provided within the flow depth. Several simulations are run from coarser to finer mesh in order to obtain mesh independency. In this case, the computational domain is smaller than Case 1 which decreases the computational time. Both uniform and non-uniform meshes are tested. For non-uniform mesh option, additional mesh plane is added to the chute surface which allowed grid refinement along this surface. As a result, even more points are provided within the flow depth compared with the uniform mesh distribution. Trials for Case 2 are shown in the Table 5.4.

Table 5.4 Summary of Grid Generation Trials for Case 2

Simulation #	Cell Size (m) x- direction	Cell Size (m) y- direction	Cell Size (m) z- direction	Total Number of Cells
NMR 1	0.050	0.050	0.050	98,640
NMR 2	0.028	0.028	0.028	506,660
NMR 3	0.023	0.023	0.023	1,004,920
NMR 4	0.016	0.016	0.016	3,027,003
NMR 5	0.016	0.016	0.010-0.022	3,027,003
NMR 6	0.013	0.013	0.008-0.018	5,340,062
NMR 7	0.011	0.011	0.006-0.016	8,949,800
NMR 8	0.010	0.010	0.005-0.015	11,862,400
NMR 9	0.009	0.009	0.004-0.014	15,220,476

As it can be seen from Table 5.4, total number of cells is less than Case 1 despite of using finer meshes for Case 2. Nine simulations are performed for Case 2 where in the first four a uniform mesh size is used in all three Cartesian coordinate directions. In the latter five simulations a uniform mesh size is used in the y direction whereas mesh size is variable in the x-z plane. Pressure head values obtained at the measurement points are compared for the experimental and numerical results with different mesh sizes in Figures 5.7 - 5.15.

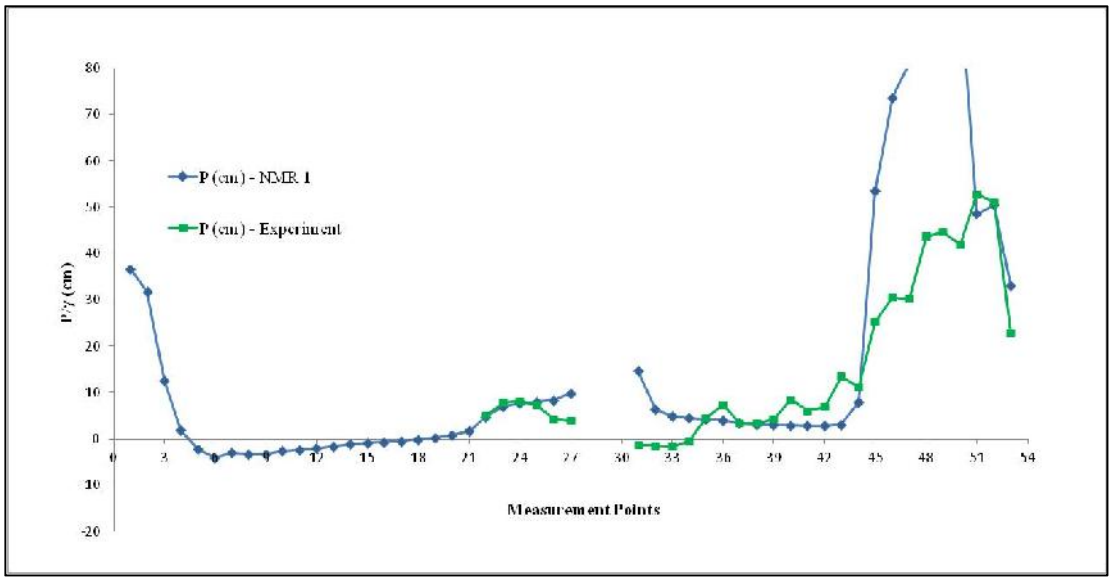

Figure 5.7 Comparison of Pressure Head Values Along The Measurement Points for NMR 1 and Experiment

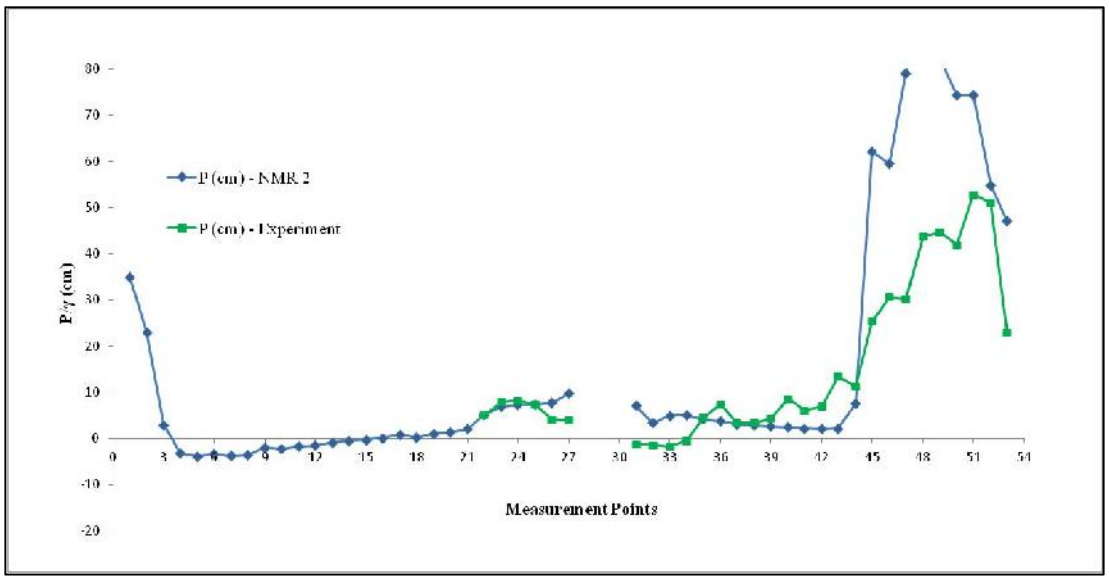

Figure 5.8 Comparison of Pressure Head Values Along The Measurement Points for NMR 2 and Experiment

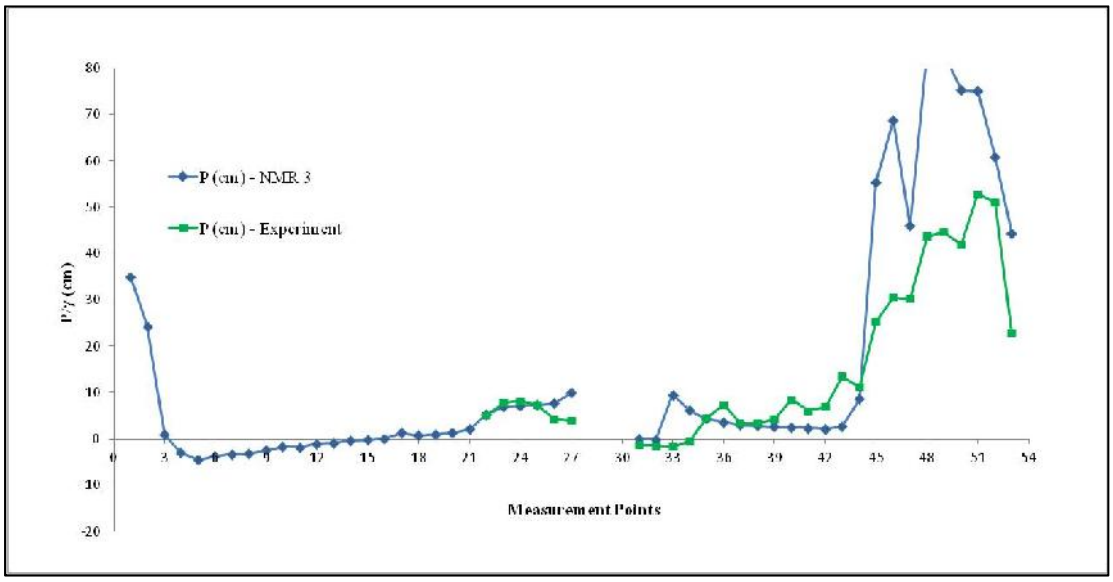

Figure 5.9 Comparison of Pressure Head Values Along The Measurement Points for NMR 3 and Experiment

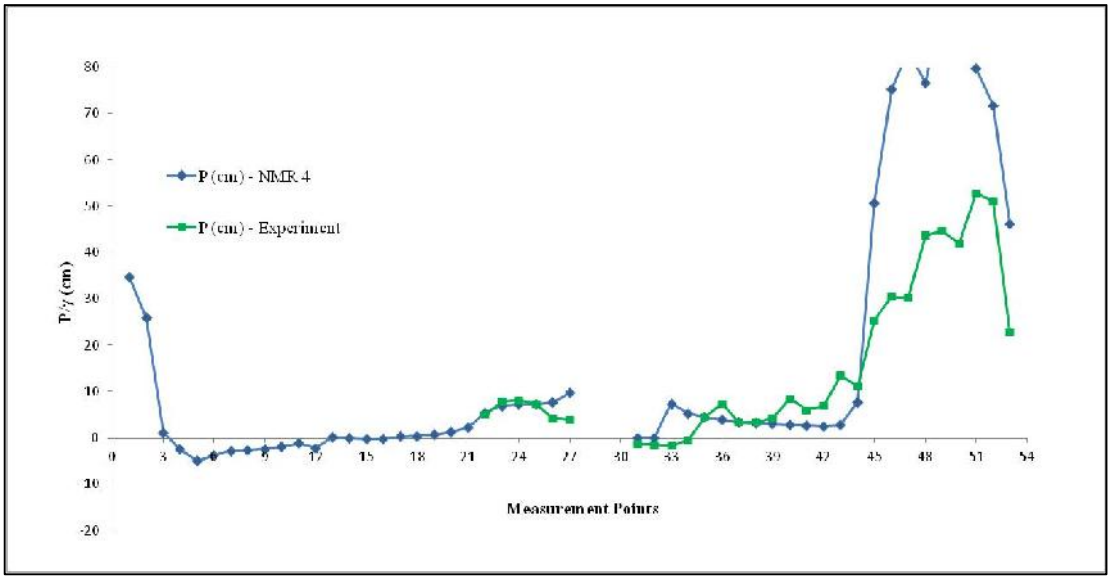

Figure 5.10 Comparison of Pressure Head Values Along The Measurement Points for NMR 4 and Experiment

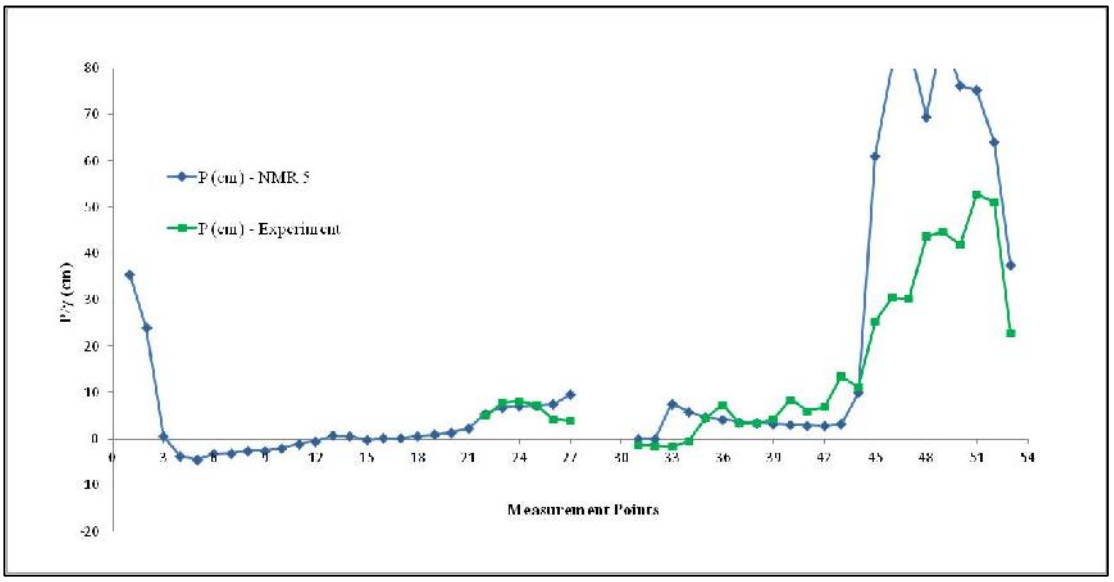

Figure 5.11 Comparison of Pressure Head Values Along The Measurement Points for NMR 5 and Experiment

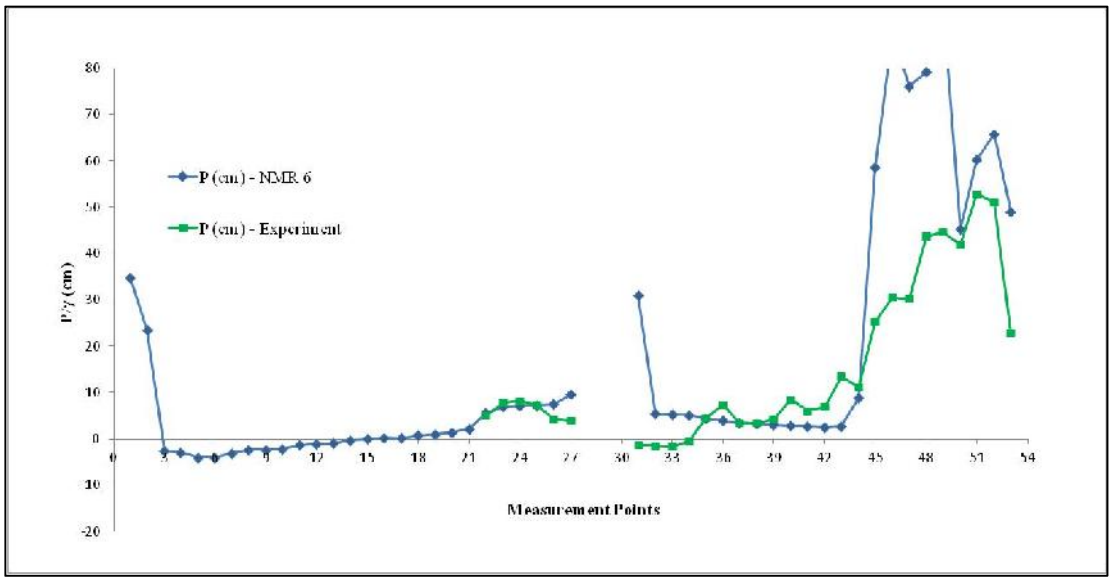

Figure 5.12 Comparison of Pressure Head Values Along The Measurement Points for NMR 6 and Experiment

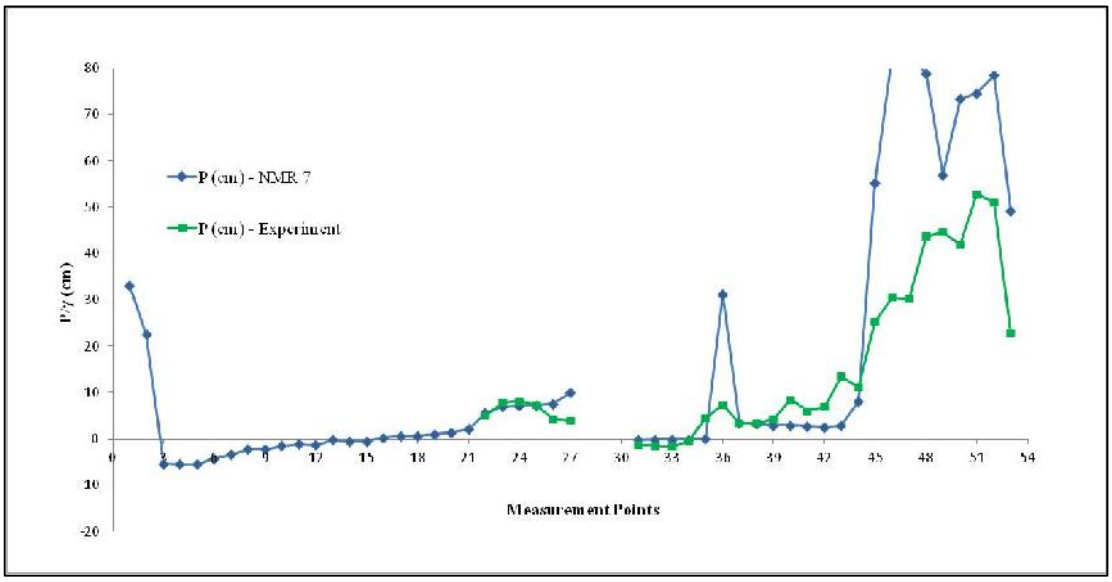

Figure 5.13 Comparison of Pressure Head Values Along The Measurement Points for NMR 7 and Experiment

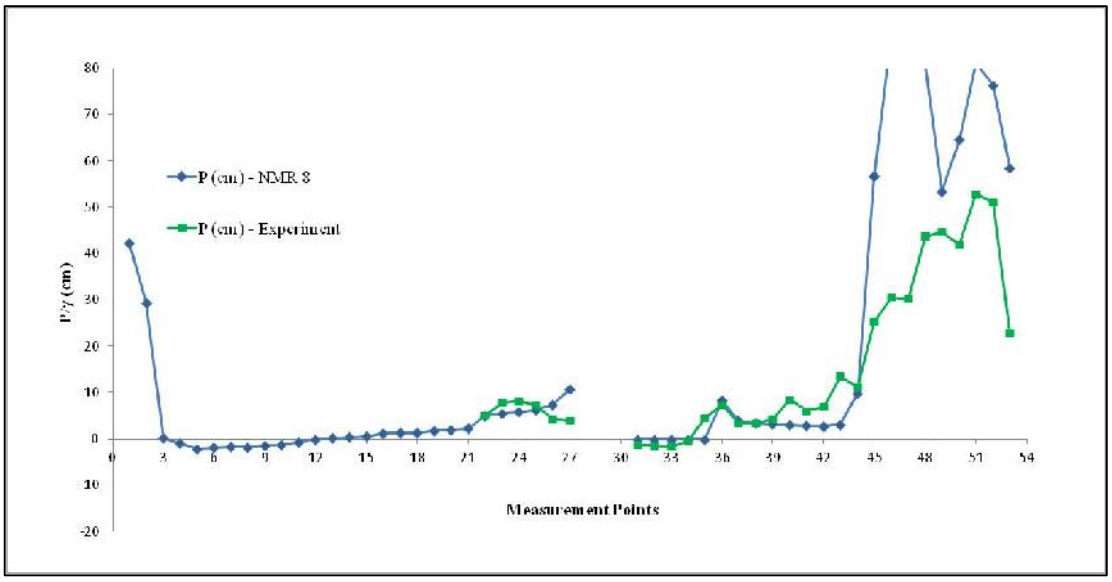

Figure 5.14 Comparison of Pressure Head Values Along The Measurement Points for NMR 8 and Experiment

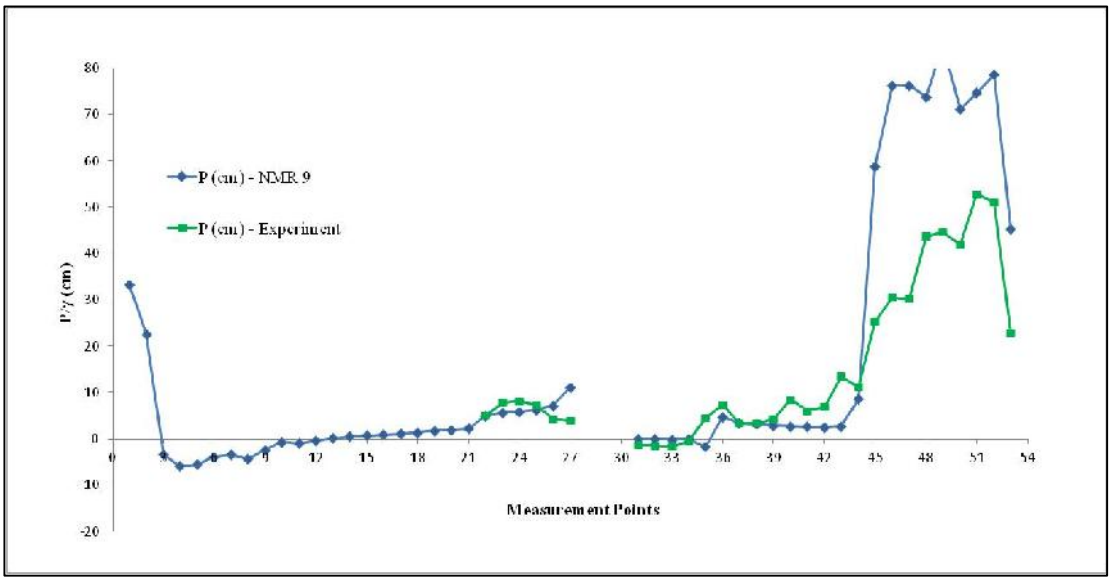

Figure 5.15 Comparison of Pressure Head Values Along The Measurement Points for NMR 9 and Experiment

Numerical model results show a good agreement with the physical model. Computational grid is aligned with the chute of spillway which allowed a better approximation of the flow along the chute. In general, pressure distribution comparison of a 3-D numerical model of Case 2 to a physical model of Laleli dam spillway (TR-5) shows relatively better agreement than Case 1. As the mesh size increases the numerical and experimental results shows a better agreement. The last two trials with the finest mesh resolution (NMR8 and NMR9) give almost the same results along the chute which is the most critical part in terms of cavitation. On the other hand there are deviations compared to the experimental results in the flip bucket part of the spillway. This is because of the high curvature within this region which could not be captured very efficiently. However the flow within the flip bucket is not critical in terms of cavitation and hence NMR8 is selected as the optimum solution for this case.

Figure 5.16 and .17 show the pressure and velocity magnitude contours respectively for simulation NMR 8. The aeration after the deflector can be clearly seen form these figures. As the water depth decreases along the chute velocity magnitude get as large as 8.5 - 9 m/s.

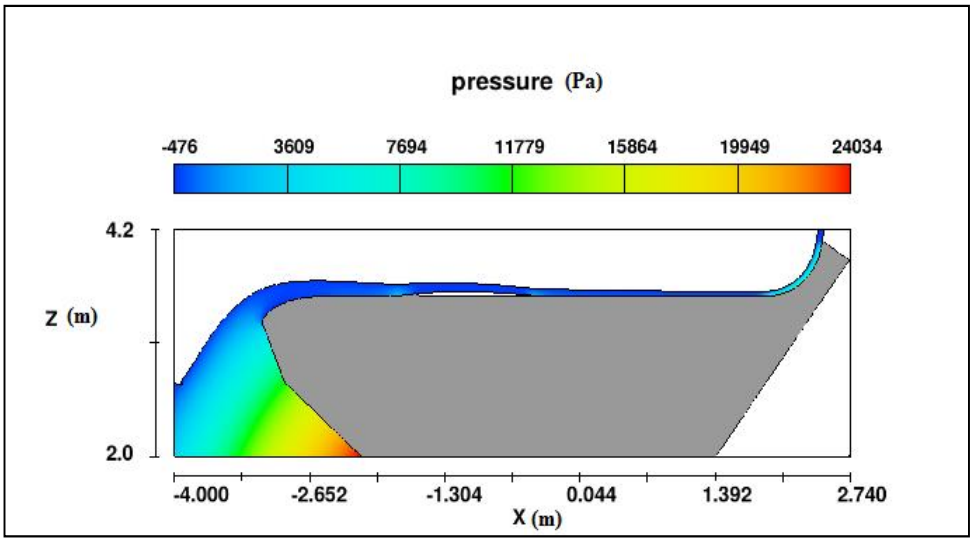

Figure 5.16 2-D Pressure Contours at Central Axis of Spillway (NMR 8)

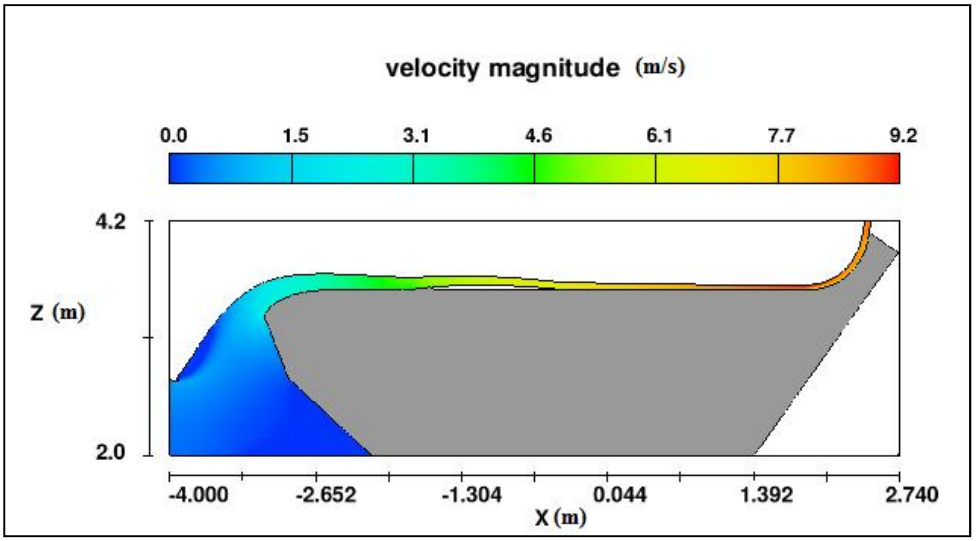

Figure 5.17 2-D Velocity Magnitude Contours at Central Axis of Spillway (NMR 8)

5.2 Air Entrainment and Scale Effects

Air entrainment effect on flow over the spillway is a very significant issue for prevention from the cavitation risk. In the experiments because of the scale effect it is very hard to estimate the correct amount of aeration that will be observed in the prototype. However in the numerical model additional simulations can be done in the prototype scale to better understand the scale effects in the aeration. In order to estimate the amount of entrained air within the flow over the spillway, a series of 3-D numerical simulations are done using air entrainment model option in Flow 3D. Qualitative description of the basic behavior of air-water flow is investigated using air entrainment model in Flow 3D. The main purpose of this model is predicting information on the air concentrations in the flow over the spillway.

Firstly, the pressure head values are compared along the spillway for simulation NMR 8 and NMR 8 with air entrainment model turned on. This comparison is shown in Figure 5.18.

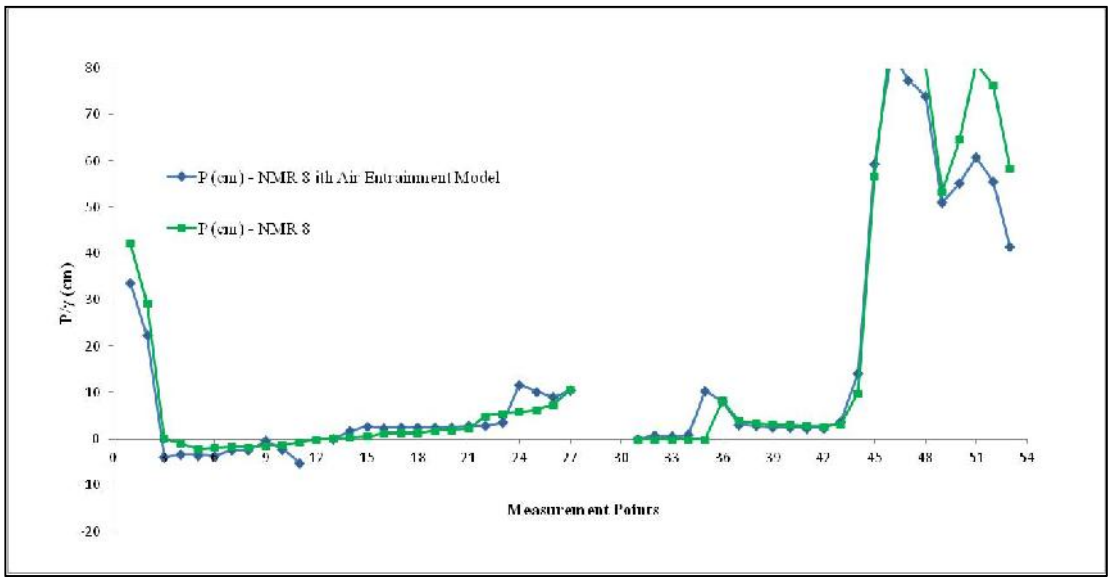

Figure 5.18 Comparison of Pressure Head Values Along The Measurement Points for NMR 8 with and without Air Entrainment Model

It is represented that there is no significant difference between NMR 8 with and without the air entrainment model in terms of the pressure heads. The reason of this situation could be the scale effect. As NMR 8 is in the model scale, the air concentrations might be so low that it is not affecting the flow. In that respect, new simulations are created in order to observe the effect of the air entrainment in the prototype scale but unfortunately no experimental data is available to compare. In the prototype simulations the same mesh used in the model is scaled up with the length ratio.

Pressure head values are converted into the prototype scale using Table 5.1 and compared with the values obtained from the prototype simulation in Figure 5.19. This figure shows that similar pressure head values are obtained at both scales.

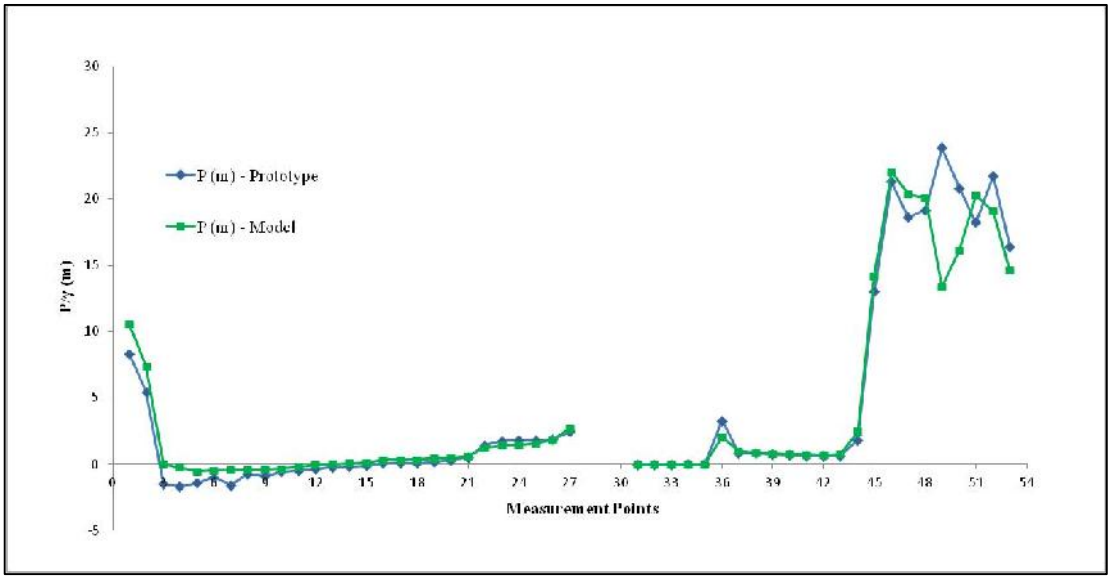

Figure 5.19 Comparison of Pressure Head Values Along The Measurement Points for NMR 8 in Model and Prototype Scale

Air entrainment option is also tried in prototype scale. Comparison of pressure distribution in prototype scale of NMR 8-Prototype with and without air entrainment option is shown in the Figure 5.20.

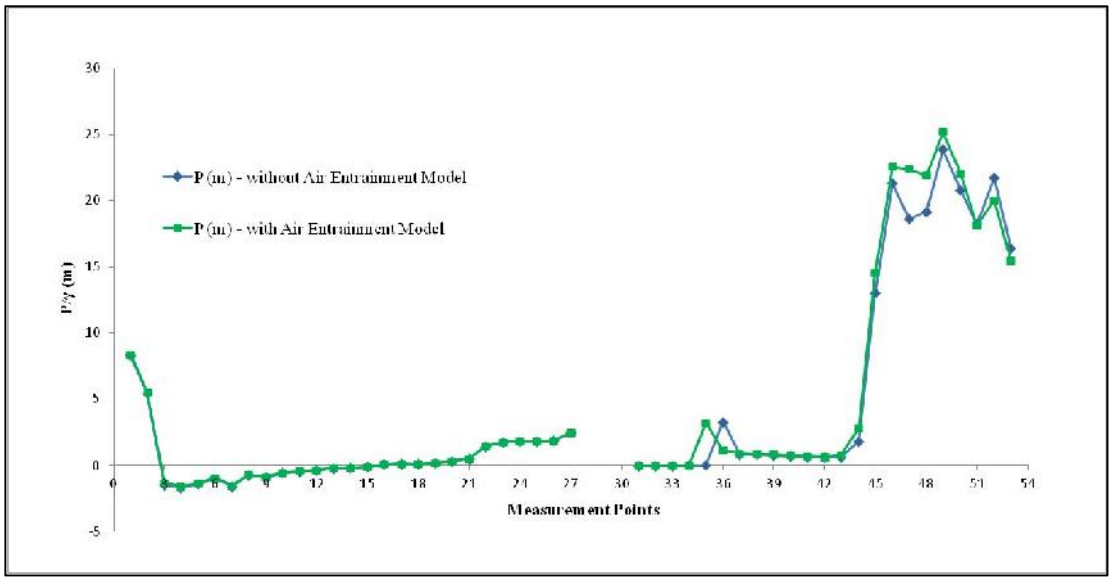

Figure 5.20 Comparison of Pressure Head Values Along The Measurement Points for NMR 8 in Prototype Scale with and without Air Entrainment Model

As it can be seen from Figure 5.20, there is no significant effect of air entrainment model on pressure head values in prototype scale too. Moreover, qualitative comparison is done between the model and prototype scale about the volume fraction of entrained air. The predicted volume fraction of entrained air for the model scale and prototype scale are shown in Figures 5.21 and 5.22 respectively.

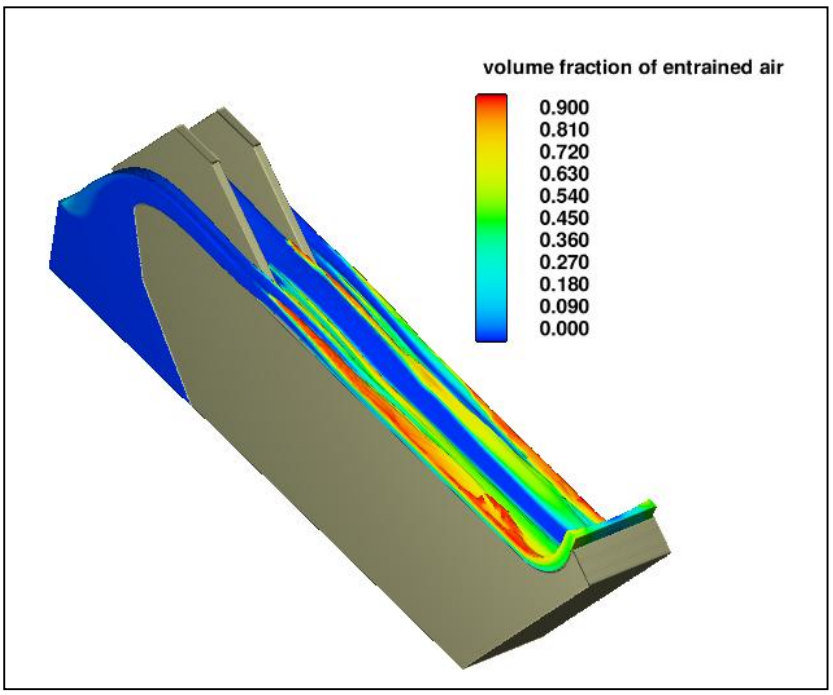

Figure 5.21 Volume Fraction of Entrained Air in Model Scale

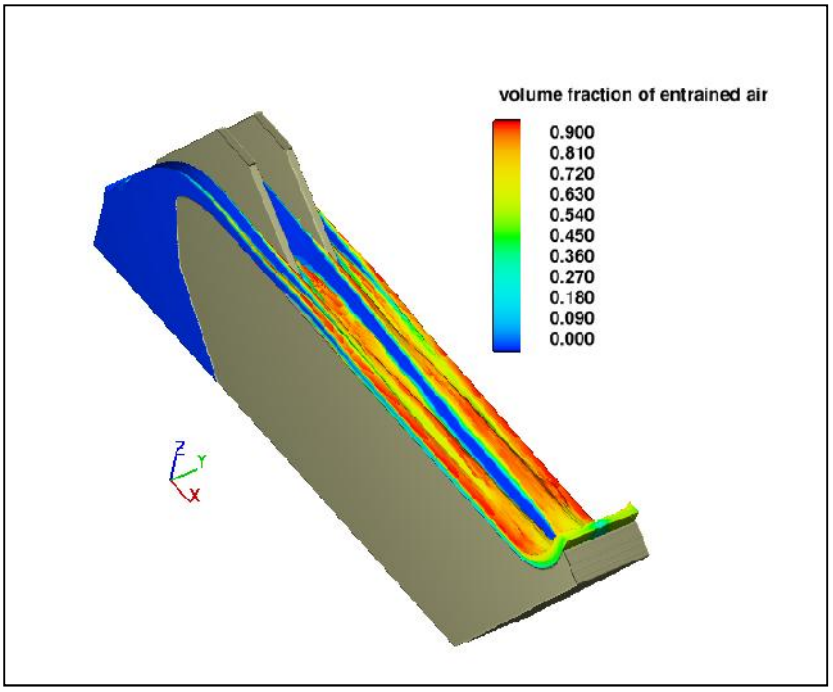

Figure 5.22 Volume Fraction of Entrained Air in Prototype Scale

In prototype scale, the volume fraction of entrained air is more than the physical model scale but the results are only qualitative and the pressure distributions do not change significantly.

Furthermore quantities of aeration (%) on selected six points are compared between the model and prototype simulations. 23rd and 27th points are located before the ramp and 34th, 37th, 40th and 42nd points are located after the ramp.

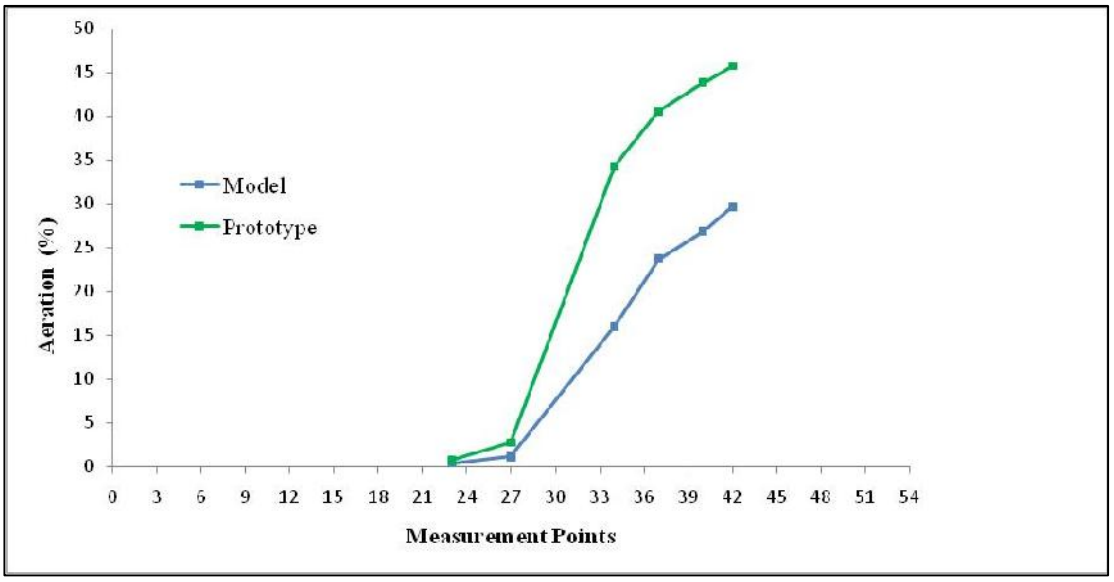

Figure 5.23 Comparison of the Aeration (%) For NMR 8 in Model and Prototype Scale

As it can be seen from Figure 5.23, the aeration increases after the ramp and the aeration (%) of prototype is more than what is observed in model scale. This is a good illustration of the scale effect in aeration amount.

5.3 Investigation of Cavitation Potential

Cavitation is one of the most common causes of failure for the spillways. Cavitation potential on the spillways is evaluated by the cavitation index, σ. Computation of σ is shown in Equation 2.1. The data required in computing the cavitation index are given below.

$P = P_{gage} + P_{atm}$

$P_{atm} = 83{,}657.40$ Pa

$P_{vapor} = 2{,}330$ Pa

$\rho_{water} = 1000$ kg/m^3

In cavitation index calculation, the all variables are converted to prototype scale using Table 5.1. Cavitation index depends on the local pressure and velocity. Based on the computed velocity and pressure distribution on spillway, the cavitation index can be calculated. The critical value of cavitation index is taken as 0.2. Cavitation risk begins if the cavitation index is smaller than 0.2. By calculating the cavitation number at the different sections of the numerical model, it is realized that cavitation may occur due to high velocities in the spillway chute.

Once the pressure distribution along the spillway surface is investigated, one can see that there are negative pressures near the crest of spillway but it is not a significant issue due to the low velocities at this region. The negative pressure has importance in terms of cavitation at sections of high velocities. Low pressure values together with high velocities occur typically along the chute of a spillway so that cavitation risk increases.

It is known that the aeration of flow over the spillway could decrease the cavitation risk. For this purpose ramps are commonly used. In the experimental model study of Aydın et al. (2012), the geometric properties of the ramp were investigated to find the optimum aeration. The scenario TR-5 was determined as a solution of the problem. In the numerical model study, scenario TR-5 is simulated and compared.

Six sections (23, 27, 34, 37, 40 and 42) are selected on the spillway and cavitation indexes are calculated at these sections. Velocity distributions in x-z plane at selected points are shown Figure 5.24 - 5.29.

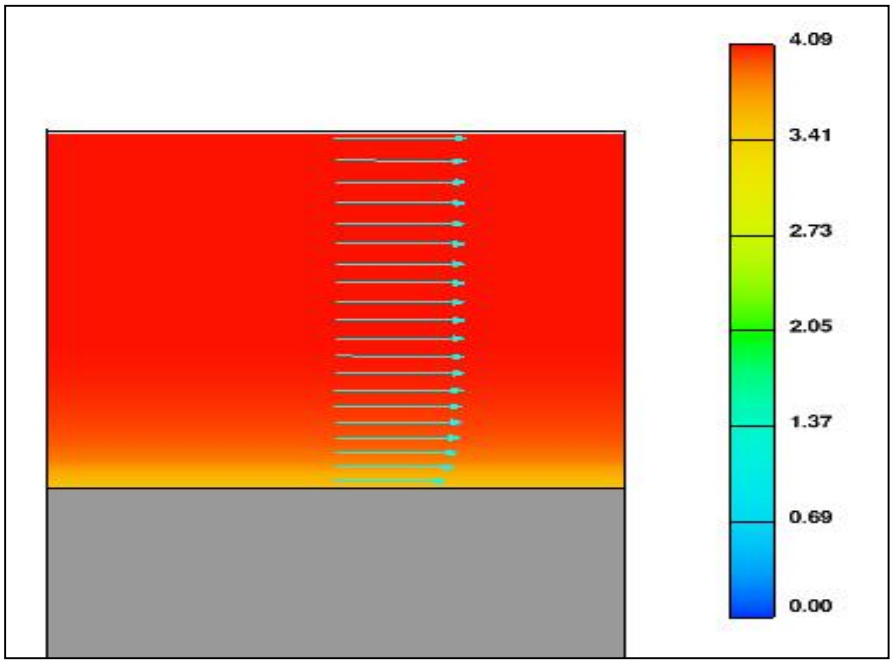

Figure 5.24 Velocity Distribution at 23rd point (x-z plane)

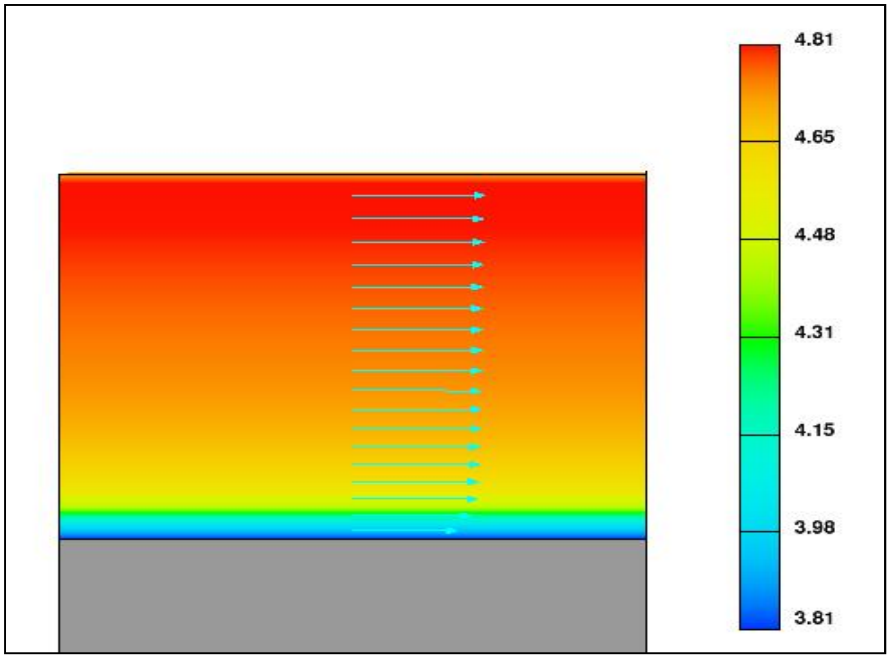

Figure 5.25 Velocity Distribution at 27th point (x-z plane)

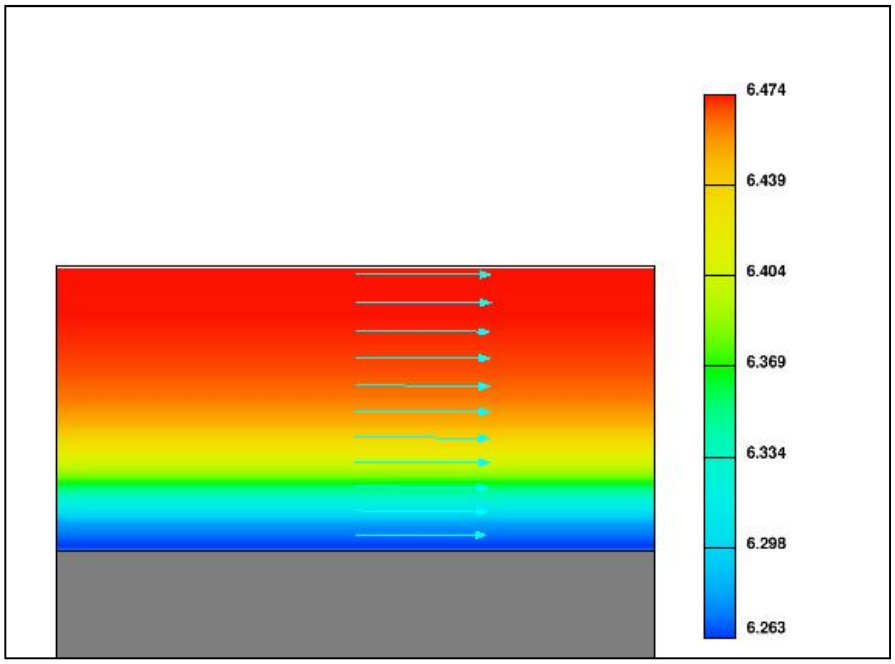

Figure 5.26 Velocity Distribution at 34th point (x-z plane)

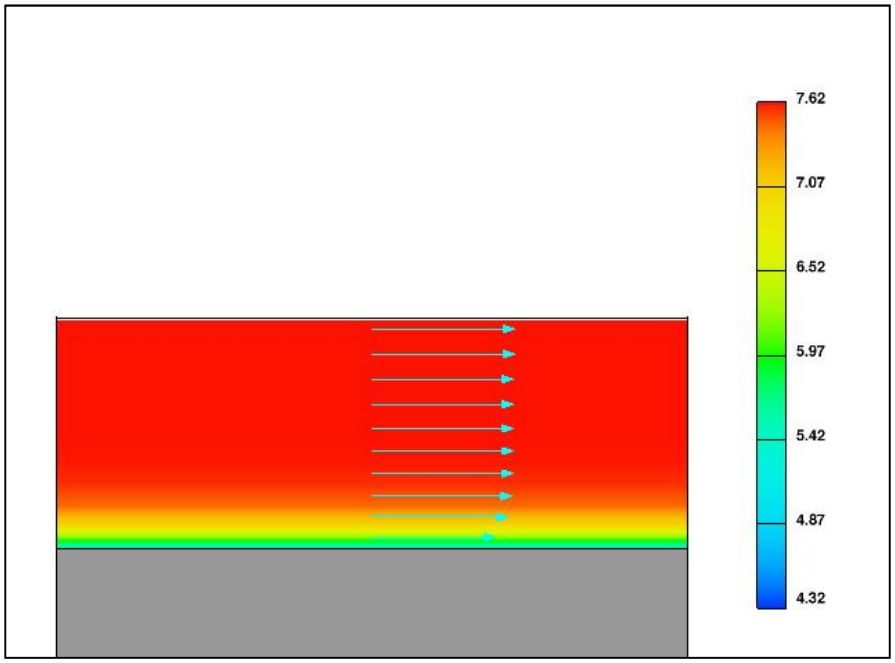

Figure 5.27 Velocity Distribution at 37th point (x-z plane)

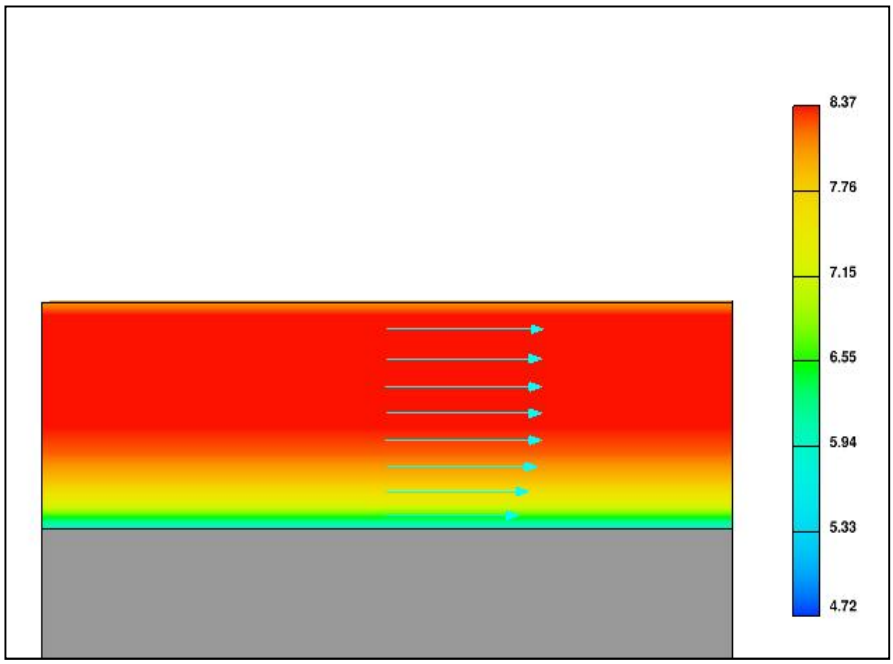

Figure 5.28 Velocity Distribution at 40th point (x-z plane)

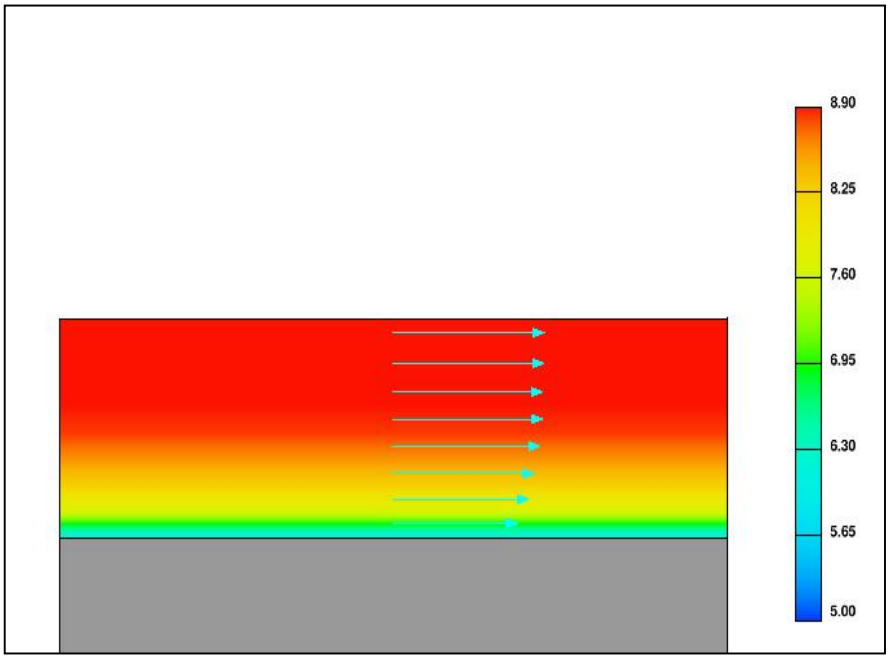

Figure 5.29 Velocity Distribution at 42nd point (x-z plane)

Depth-averaged velocities are used while computing the cavitation indexes whereas pressure values are recorded at the surface of the spillway.

Table 5.5 shows the calculation of cavitation indexes and Figure 5.30 shows the comparison of cavitation indexes for TR-5 case both for numerical and physical model.

Table 5.5 Cavitation Indexes for TR-5 Using Depth-Averaged Velocity

Points	Pressure-Model (Pa)	Equivalent Pressure-Prototype (Pa)	Dept-Averaged Velocity-Model (m/s)	Equivalent Velocity-Prototype (m/s)	Cavitation Index
23	546.66	13666.48	4.01	20.04	0.47
27	1052.86	26321.53	4.70	23.49	0.39
34	-9.92	-248.00	6.41	32.05	0.16
37	9628.56	9628.56	7.33	36.64	0.14
40	291.75	7293.69	7.94	39.69	0.11
42	269.03	6725.80	8.26	41.32	0.10

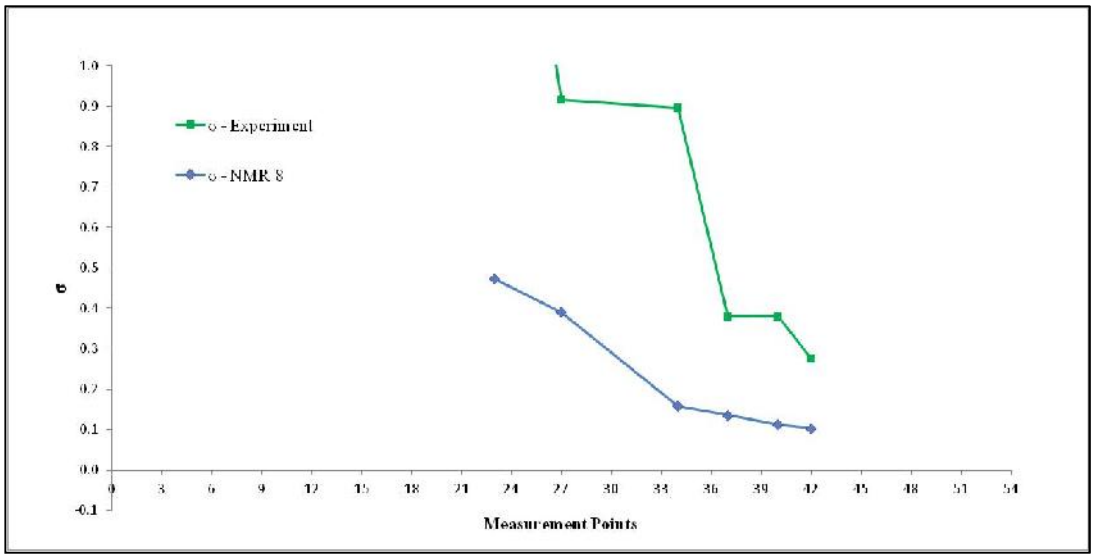

Figure 5.30 Comparison of the Experimental and the Numerical Cavitation Index Values for TR-5

The numerical results of cavitation number do not agree well with measurements due to the differences in the velocity magnitudes between the experiment and the simulation as shown in Figure 5.31.

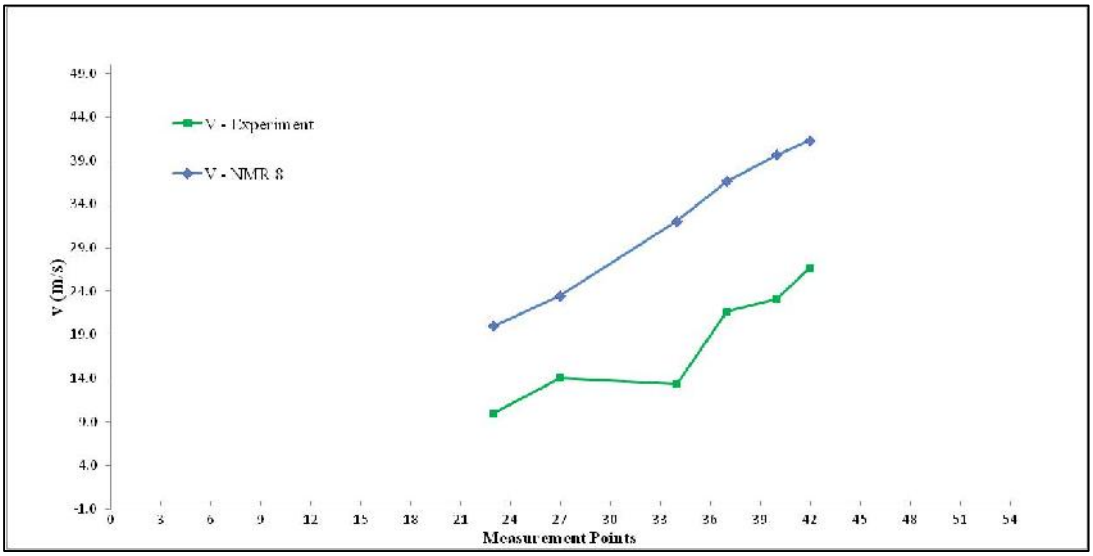

Figure 5.31 Comparison of the Depth-Averaged Velocity Values for TR-5

In the physical model study, the velocity was calculated from section averaged measurements which is obtained from Equation 5.1.

$$Q = b * y * V \quad (5.1)$$

Q: Discharge (m^3/s)

b: width of the spillway (m)

y_{av} : section-averaged depth (m)

V : section-averaged velocity (m/s)

Same procedure is applied in the numerical model in order to calculate the section-averaged velocity. The section averaged depth is calculated by integration in the width of spillway section. Table 5.6 shows the section-averaged velocities and Figure 5.32 shows the comparison of section-averaged velocities.

Table 5.6 Section-Averaged Velocity Computation

Points	Discharge-Model (m^3/s)	Width-Model (m)	Section-Averaged Depth-Model (cm)	Section-Averaged Velocity (m/s)	Equivalent Section-Averaged Velocity-Prototype (m/s)
23	0.16	0.80	14.1	1.45	7.27
27			11.6	1.77	8.84
34			10.3	1.99	9.95
37			5.7	3.60	17.98
40			5.2	3.94	19.71
42			4.9	4.18	20.92

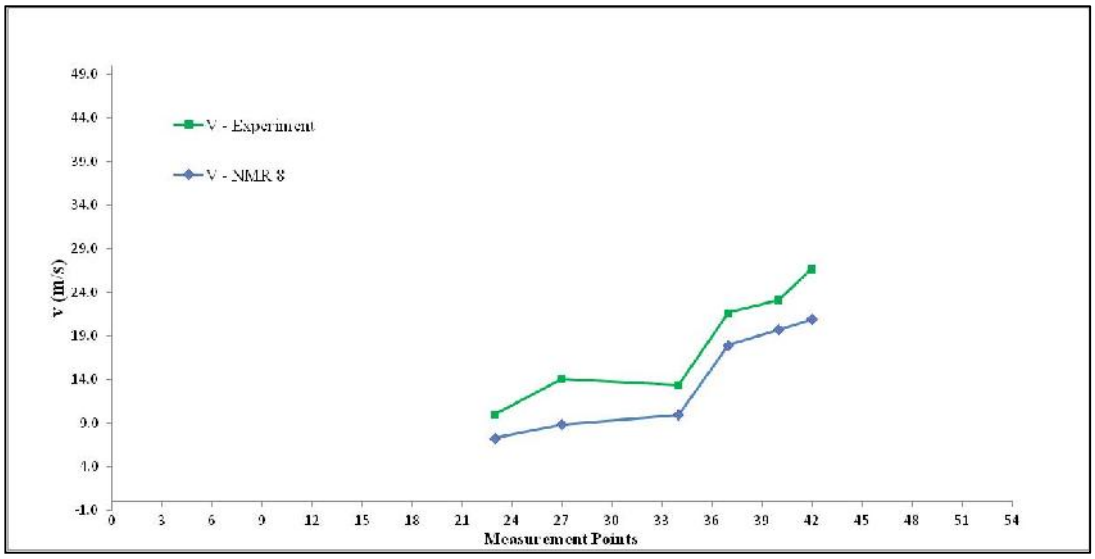

Figure 5.32 Comparison of the Section-Averaged Velocity Values for TR-5

According to the computation of cavitation indexes using section-averaged velocities, the cavitation indexes are close to each other and a good agreement is obtained between the numerical model and the physical model. The results are shown in Table 5.7 and Figure 5.33.

Table 5.7 Cavitation Indexes for NMR 8 Using Section-Averaged Velocity

Points	Pressure-Model (Pa)	Equivalent Pressure-Prototype (Pa)	Velocity-Model (m/s)	Equivalent Velocity-Prototype (m/s)	Cavitation Index
23	546.66	13666.48	1.45	7.27	3.61
27	1052.86	26321.53	1.77	8.84	2.75
34	-9.92	-248.00	1.99	9.95	1.64
37	9628.56	9628.56	3.60	17.98	0.56
40	291.75	7293.69	3.94	19.71	0.46
42	269.03	6725.80	4.18	20.92	0.40

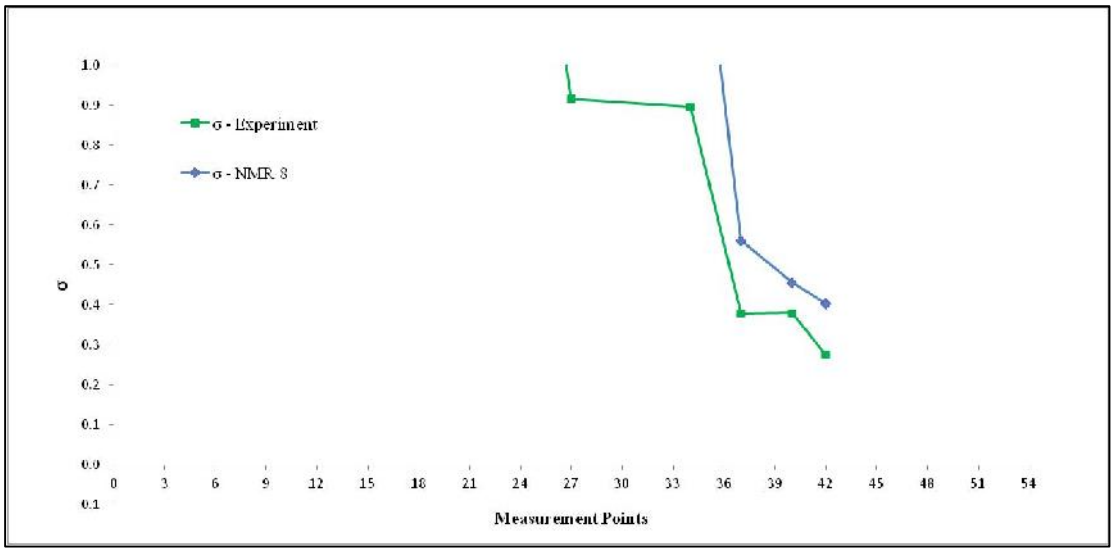

Figure 5.33 Comparison of the Experimental and the Numerical Cavitation Index Values for TR-5

CHAPTER 6

CONCLUSIONS

The role of numerical modeling has been increasing in the hydraulic design of the spillways. Although the numerical simulations could provide a cost effective alternative to physical model tests, results of the numerical models should be verified. The validation is generally provided by comparing the results of the numerical model to the results of a physical model. Although CFD tools still have some limitations such as long run times, and numerical instabilities, they are more economical and can provide more details about hydraulic characteristics than a scaled physical model. Furthermore, many more scenarios could be easily tested with easy modifications to the numerical model. Thus, the numerical models have the flexibility in studying in different flow phenomena. However, it is important to select an appropriate mesh, with correct initial and boundary conditions for an accurate numerical solution.

To obtain the hydraulic parameters of Laleli dam spillway, Flow 3D is used as a CFD tool. The numerical solutions given by Flow 3D are investigated and results are compared with the 1:25 scaled physical model results. In the solver process, Flow 3D is programmed to use the Reynolds Averaged Navier-Stokes Equations approach coupled with the RNG closure model as a turbulence model. Air entrainment model is also tested. One fluid incompressible flow approach is used for all simulations. The following conclusions can be reached from the present study:

1. CFD is an effective tool for analyzing free surface flows over spillways. A lot of studies about spillway have been done. A validation of numerical model using a physical model provides additional confidence in the results. CFD tools can be used as a design alternative of hydraulic structures together with suitable physical model test for validation.

It is important to have a grid independent solution in a numerical study. In the grid selection and mesh refinement stage, Flow 3D's add restart option is used in order to increase the time efficiency of the computations and provide good initial condition.

2. In flow over the spillway, a high mesh resolution near the wall is a significant issue to advect the flow accurately and compute the pressure distribution.

3. Determining air entrainment effect on the numerical model is extremely challenging. In Flow 3D, there is an air entrainment model. This model predicts the volume of air in the flow with one phase solution qualitatively and qualitatively. It is clearly shown that aeration amounts are much larger in the prototype scale compared with the model scale. Unfortunately, there was no experimental data on aeration quantities in the physical model study to compare simulation results.

4. The effect of entrained air on the pressure distribution over the spillway is negligible in the numerical model when air entrainment model is used.

5. Pressure distribution recorded over the spillway is very similar in the model and prototype scales.

6. Cavitation indexes are computed on selected sections using both depth averaged velocities and section averaged velocities. Good agreement is obtained between the numerical model and the experiment using section averaged velocities in computing cavitation indexes.

REFERENCES

Aydın, I., Göğüş, M., Altan-Sakarya, B.A., Köken, M., (2012), Laleli Barajı Ve Hidroelektrik Santrali Dolusavak Hidrolik Model Çalışmaları, İnşaat Mühendisliği Bölümü, Hidromekanik Laboratuarı, ODTÜ.

Azmoudeh, M.H.E., Kamanbedast, A.A., (2013), Determine The Appropriate Location Of Aerator System On Gotvandolidam's Spillway Using Flow 3D, American-Eurasian J. Agric. & Environ. Sci., 13 (3): 378-383.

Bhajantri, M.R., Eldho, T.I., Deolalikar, P.B., (2006), Two-Dimensional Free Surface Flow Over A Spillway- A Numerical Model Case Study, Journal of Hydraulic Engineering, ISH, 12:2, 7-24.

Computational Fluid Dynamics Software – Flow 3D from Flow Science, CFD. www.flow3d.com

Daneshkhah, A., Vosoughifar, H., (2012), Solution Of Flow Field Equations To Investigate The Best Turbulent Model Of Flow Over A Standard Ogee Spillway In Finite Volume Method.

Dargahi, B., (2006), Experimental Study And 3D Numerical Simulations For A Free-Overflow Spillway, Journal of Hydraulic Engineering, ASCE, Vol. 132, No. 9.

Falvey, H.T., (1990), Cavitation in Chutes and Spillways.

Flow 3D Lecture Notes, Hydraulic Training Class, (2012).

Flow 3D, v10.1 User Manuel, (2012).

Flow 3D, Advanced Hydraulics Training, (2012).

Hirsch, C., (1988), Numerical Computation of Internal and External Flows, Volume 1: Fundamentals of Numerical Discretization.

Hirt, J.E., Nichols, B.D. (1981), Volume Of Fluid (VOF) Method For The Dynamics Of Free Boundaries, Journal of Computational Physics 39,201.

Ho, D.K.H., Cooper, B.W., Riddette, K.M., Donohoo, S.M., (2006), Application Of Numerical Modeling To Spillways In Australia, Dams and Reservoirs, Societies and Environment in the 21st Century- Berga et al.

Ho, D., Boyes, K., Donohoo, S., Cooper, B., (2003), "Numerical Flow Analysis For Spillways, 43nd Ancold Conference, Hobart, Tasmania.

Jacobsen, J., Olsen, N.R.B., (2009), Numerical Modeling Of The Capacity For A Complex Spillway, Water Management 163, Issue WM6.

Johnson, M.C., Savage, B.M., (2001), Flow Over Ogee Spillway: Physical And Numerical Model Case Study, Journal of Hydraulic Engineering, ASCE, Vol. 127, No. 8.

Johnson, M.C., Savage, B.M., (2006), Physical And Numerical Comparison Of Flow Over Ogee Spillway In The Presence Of Tailwater, Journal of Hydraulic Engineering, ASCE, Vol. 132, No. 12.

Kim, S., An, S., (2010), Improvement Of Hydraulic Stability For Spillway Using CFD Model, International Journal of the Physical Sciences Vol. 5(6), pp. 774-780.

Kim, D.G., Park, J.H., (2005), Analysis Of Flow Structure Over Ogee-Spillway In Consideration Of Scale And Roughness Effects By Using CFD Model, Journal Of Civil Engineering, KSCE, Vol. 9, No. 2., pp. 161-169.

Morales, V., Tokyay, T.E., Garcia, M., (2012), Numerical Modeling Of Ogee Crest Spillway And Tainter Gate Structure Of A Diversion Dam On Canar River, Ecuador, XIX International Conference On Water Resources.

Olsen, N.R.B., Kjellesvig, H.M., (1998), Three-Dimensional Numerical Flow Modeling For Estimation Of Spillway Capacity, Journal of Hydraulic Research, 36:5, 775-784.

Song, C. C. S., Zhou, F., (1999), Simulations Of Free Surface Flow Over Spillway, Journal of Hydraulic Engineering, ASCE, Vol. 125, No. 9.

Stamou, A.I., Chapsas, D.G., Christodoulou, G.C., (2008), 3-D Numerical Modeling Of Supercritical Flow In Gradual Expansions, Journal of Hydraulic Research, 46:3, 402-409.

Teklemariam, E., Korbaylo, B.W., Groeneveld, J.L., Fuchs, D.M., (2002), Computational Fluid Dynamics: Diverse Applications In Hydropower Project's Design and Analysis, CWRA 55th Annual Conference.

Unami, K., Kawachi, T., Babar, M.M., Itagaki, H., (1999), Two-Dimensional Numerical Model Of Spillway Flow, Journal of Hydraulic Engineering, ASCE, Vol. 125, No. 4.

United States Department of the Interior Bureau of Reclamation, (1987), Design of Small Dams, Third Edition.

Versteeg, H.K., Malalasekera, W., (2007), An Introduction to Computational Fluid Dynamics The Finite Volume Method, Second Edition.

Yakun, G., Xianyun, W., Chigong, W., Duo, F., (1998), Numerical Modeling Of Spillway Flow With Free Drop And Initially Unknown Discharge, Journal of Hydraulic Research 36:5, 785-801.

Zhenwei, M., Zhiyan, Z., Tao, Z., (2012), Numerical Simulation Of 3-D Flow Field Of Spillway Based On VOF Method, 2012 International Conference On Modern Hydraulic Engineering, SciVerse ScienceDirect, Procedia Engineering 28 (2012) 808-812.